STEM CELLS AND DEVELOPMENT
Volume 24, Number 21, 2015
© Mary Ann Liebert, Inc.
DOI: 10.1089/scd.2015.0197

Angiogenic Potential and Secretome of Human Apical Papilla Mesenchymal Stem Cells in Various Stress Microenvironments

Athina Bakopoulou,[1,2] Aristeidis Kritis,[3] Dimitrios Andreadis,[4] Eleni Papachristou,[1] Gabriele Leyhausen,[2] Petros Koidis,[1] Werner Geurtsen,[2] and Asterios Tsiftsoglou[5]

Stem cells from the apical papilla (SCAP) of human adult teeth are considered an accessible source of cells with angiogenic properties. The aims of this study were to investigate the endothelial transdifferentiation of SCAP, the secretion of pro- and antiangiogenic factors from SCAP, and the paracrine effects of SCAP when exposed to environmental stress to stimulate tissue damage. SCAP were exposed to serum deprivation (SD), glucose deprivation (GD), and oxygen deprivation/hypoxia (OD) conditions, individually or in combination. Endothelial transdifferentiation was evaluated by in vitro capillary-like formation assays, real-time polymerase chain reaction, western blot, and flow cytometric analyses of angiogenesis-related markers; secretome by antibody arrays and enzyme-linked immunosorbent assays (ELISA); and paracrine impact on human umbilical vein endothelial cells (HUVECs) by in vitro transwell migration and capillary-like formation assays. The short-term exposure of SCAP to glucose/oxygen deprivation (GOD) in the presence, but mainly in deprivation, of serum (SGOD) elicited a proangiogenesis effect indicated by expression of angiogenesis-related genes involved in vascular endothelial growth factor (VEGF)/VEGFR and angiopoietins/Tie pathways. This effect was unachievable under SD in normoxia, suggesting that the critical microenvironmental condition inducing rapid endothelial shift of SCAP is the combination of SGOD. Interestingly, SCAP showed high adaptability to these adverse conditions, retaining cell viability and acquiring a capillary-forming phenotype. SCAP secreted higher numbers and amounts of pro- (angiogenin, IGFBP-3, VEGF) and lower amounts of antiangiogenic factors (serpin-E1, TIMP-1, TSP-1) under SGOD compared with SOD or SD alone. Finally, secretome obtained under SGOD was most effective in inducing migration and capillary-like formation by HUVECs. These data provide new evidence on the microenvironmental factors favoring endothelial transdifferentiation of SCAP, uncovering the molecular mechanisms regulating their fate. They also validate the angiogenic properties of their secretome giving insights into preconditioning strategies enhancing their therapeutic potential.

Introduction

Angiogenesis, the process of generating new blood vessels from existing ones [1], is one of the major challenges for regeneration of various damaged tissues and organs by breathing life into constructed tissue-engineered substitutes [2]. Understanding the molecular mechanisms regulating neoangiogenic processes in various stress microenvironments frequently present in injury sites (deprivation of oxygen and/or nutrients) is critical for optimizing methods used for cell-based tissue regeneration of pathologies attributed to severe ischemia, such as heart infarcts, diabetic extremities, cerebral ischemia/stroke areas, and wound healing. Such an approach would be also highly valuable for the regeneration of dental pulp, the innervated and heavily vascularized core of the tooth, having an average capillary density higher than most other tissues and a blood flow of 50 mL/min/100 g of pulp tissue [3].

Angiogenesis is a complex multistep process regulated by the balance between inductive and inhibitory signals and their cascade pathways [1,3]. In adults, the endothelium and supportive cells of blood vessels (ie, pericytes) are usually

[1]Department of Fixed Prosthesis and Implant Prosthodontics, School of Dentistry, Aristotle University of Thessaloniki (A.U.TH.), Thessaloniki, Greece.
[2]Department of Conservative Dentistry, Periodontology and Preventive Dentistry, Hannover Medical School (MHH), Hannover, Germany.
[3]Department of Physiology and Pharmacology, School of Medicine, Aristotle University of Thessaloniki (A.U.TH.), Thessaloniki, Greece.
[4]Department of Oral Medicine and Pathology, School of Dentistry, Aristotle University of Thessaloniki (A.U.TH.), Thessaloniki, Greece.
[5]Laboratory of Pharmacology, School of Pharmaceutical Sciences, Aristotle University of Thessaloniki (A.U.TH.), Thessaloniki, Greece.

in a quiescent state. At first, angiogenesis is triggered in response to tissue or systemic stimuli, including hypoxia and inflammation. It initiates by blood vessel destabilization induced by vascular endothelial growth factor (VEGF) and angiopoietin-2 (Ang-2). It continues with extracellular matrix (ECM) degradation by several enzymes, such as matrix metalloproteinases (MMPs), chymases, and heparanases. This enzymatic activation leads to the release of growth factors, such as basic fibroblast growth factor (bFGF), VEGF, and insulin-like growth factor 1 (IGF-1) sequestered within ECM [4]. In a second step, proliferating endothelial cells (ECs) migrate to distant sites to form new blood vessels. This complex process is regulated by several stimulators [including VEGF and its receptors VEGF-R1 and -R2, Angs-1 and -2 and their receptor Tie-2, bFGF, platelet-derived growth factor (PDGF), IGF-1, hepatocyte growth factor (HGF), tumor necrosis factor alpha, transforming growth factor beta 1 (TGF-β1), integrins $a_v\beta_3$ and $a_5\beta_3$, urokinase-type plasminogen activator (uPA), MMPs, PECAM-1, VE-cadherin, and nitric oxide] as well as inhibitors [thrombospondins (TSP-1 and -2), endostatin, angiostatin, vasostatin, platelet factor 4 (PF4), interferons-β and -γ, and tissue inhibitors of MMPS (TIMPs)] [5]. Finally, angiogenesis is completed by the recruitment of smooth muscle cells to stabilize the newly formed blood vessels. Factors, such as PDGF-BB, Ang-1, Tie-2, TGF-β1, TGF-β-R2, and endoglin, are among the key players in this final step [6].

Previous reports have shown that transplanted mesenchymal stem cells from bone marrow (BM-MSCs) may promote angiogenesis either through their endothelial transdifferentiation and active participation in new blood vessel formation [7,8] or through the secretion of prosurvival and angiogenic factors promoting endogenous angiogenesis through an autocrine, paracrine, or juxtacrine effect [9]. The plethora of secreted trophic and immunomodulatory cytokines produced by MSCs (MSC secretome) have already been used to treat cardiovascular diseases [10] and proposed for the treatment of traumatic brain injuries [11], bone regeneration [12], or chronic wounds [13]. In addition to these two mechanisms, dental pulp stem cells (DPSCs) have been also shown to possess a functional role as pericytes, able to guide and support ECs to form new blood vessels through a VEGF-2-dependent mechanism [14].

MSCs have been isolated from various dental sources, among them the dental pulp of exfoliated [stem cells from human exfoliated deciduous teeth (SHED)] and permanent teeth [dental pulp stem cells (DPSCs)] and the apical papilla of developing teeth [stem cells from the apical papilla (SCAP)] [15]. Evidence indicates these cells residing in perivascular niches of the human pulp/apical papilla, with positivity for STRO-1 and CD146 [16]. In vitro studies have shown that coculture of DPSCs with ECs significantly improves the angiogenic potential of ECs [17], especially under hypoxic conditions [18]. Other studies have shown the in vitro transdifferentiation capacity of SHED into ECs [19] through activation of MEK1/ERK signaling [20], while some in vivo studies have demonstrated their potential to promote neovascularization in myocardial infarction and hind limb ischemia small animal models [21,22].

Recently, it has been shown that DPSCs and SCAP secrete under serum deprivation (SD) conditions several pro- and antiangiogenic factors able to promote migration and tubule formation by ECs and to induce new blood vessel formation in a chicken chorioallantoic membrane model [23,24]. Secretion of angiogenic factors by pulp cells may be modulated by local microenvironments, such as the aftermath of experimental pulp injury, exposure to toxic resinous monomers released by restorative materials, or hypoxia-related conditions encountered in clinical situations, such as carious or traumatic pulp injuries, orthodontic movement, or reimplantation of avulsed teeth [25].

Despite the considerable accumulated knowledge on the endothelial transdifferentiation potential of dental MSCs and the angiogenic properties of their secretome, not enough is well understood on how do stress conditions pertaining to in vivo situations involving damaged tissues affect their potential for angiogenesis. Similarly, little information exists on the effects of paracrine action of dental MSCs to modulate the local microenvironment at injury sites.

In this context, the present study aimed to investigate the impact of various stress microenvironmental factors [including serum deprivation (SD), glucose deprivation (GD), and hypoxia/oxygen deprivation (OD), separately or in combination] on the endothelial transdifferentiation capacity of human SCAP and the angiogenic properties of their secretome. SCAP were selected as representing less mature dental MSCs residing in a heavily vascularized tissue [26], offering an attractive cell source for pulp or other tissue regeneration.

Materials and Methods

Establishment of SCAP cultures

SCAP cultures were established from the apical papilla of human developing third molars obtained from three young healthy donors aged 15, 17, and 19 years. The collection of the samples was performed according to the guidelines of the Institutional Review Board, and all donors or their parents signed an informed consent. SCAP cultures were established using the enzymatic dissociation method, as previously described [26]. Briefly, impacted third molars at the stage of root development (two thirds of the root completed) were disinfected and cut through the cementum–enamel junction to reveal the pulp chamber. Then, the dental pulp (white part) and the apical papilla (red part) were recovered as a whole segment through the coronal part of the tooth, and then separated from each other with a scalpel. To ensure that only the apical papilla was used for the establishment of SCAP cultures, the section was performed toward the apical papilla part, while the pulp part was discarded. The papilla tissue was then minced into small segments and digested in a solution of 3 mg/mL collagenase type I and 4 mg/mL dispase (both from Invitrogen) for 1 h at 37°C. Cells were expanded with alpha minimum essential (aMEM) culture medium supplemented with 15% fetal bovine serum (FBS), 100 U/mL penicillin, 100 mg/mL streptomycin, and 0.25 mg/mL amphotericin B (all from Invitrogen) and 100 mM L-ascorbic acid phosphate (Sigma-Aldrich) [complete culture medium (CCM)] and incubated at 37°C in 5% CO_2. Cultured SCAP in passage numbers from two to six derived from three healthy donors were used for all experiments.

Characterization of SCAP cultures with flow cytometry

Before using SCAP for experiments, cells at passage 2 were analyzed by flow cytometry for several markers known

to be expressed on mesenchymal (CD90/Thy-1, CD73, STRO-1, CD146/MUC18, CD24, CD34, CD81-TAPA, CD49f/a6-integrin, CD29/b1-integrin, CD51/av-integrin, CD166/ALCAM), endothelial (CD105/endoglin, CD106/VCAM), neural (CD271/NGFR, nestin), hematopoietic (CD45, CD117/c-Kit), and embryonic (Nanog, Oct3/4, SSEA-1, -3, -4, -5, TRA-1-60, and TRA-1-81) stem cells, as previously described [26]. Cells were trypsinized, washed with phosphate-buffered saline (PBS), and then stained with the following fluorochrome-conjugated mouse anti-human antibodies: CD90-FITC (fluorescein isothiocyanate) CD73-PE (phycoerythrin), STRO-1-FITC, CD146-PE, CD24-APC (allophycocyanin), CD34-APC, CD81-FITC, CD49f-APC, CD29-APC, CD51-PE, CD166-PE, CD105-FITC, CD106-APC, SSEA-1-PE, SSEA-3-PE, SSEA-4-FITC, SSEA-5-APC (all from BioLegend), TRA-1-60-PE, TRA-1-81-APC, CD271-PE, and CD45-PE (all from BD Biosciences).

For intracellular staining for Nanog, Oct3/4, and nestin, cells were first fixed with a 4% paraformaldehyde buffer, permeabilized with a 0.1% saponin buffer (both from BD Biosciences), and then stained with the mouse anti-human antibodies Oct3/4-Alexa Fluor 647, Nanog-PE (both from BioLegend), and nestin-APC (R&D Systems). Analysis was performed with a BD LSR II Flow Cytometer (BD Biosciences). A total of 100,000 events were acquired for each sample. Data were analyzed using Summit 5.1 software.

Evaluation of the endothelial transdifferentiation potential of SCAP under normoxic conditions

In an initial series of experiments, the potential of SCAP to transdifferentiate into endothelial-like cells after exposure to angiogenic media was evaluated. SCAP were seeded at 3×10^5 cells/well with CCM on collagen I (rat tail collagen I; BD Biosciences)-coated six-well plates and allowed to reach confluency ($\sim 10^6$ cells) for 3 days. Then, cells were exposed to M199 medium, supplemented with 5% FBS, 1% antibiotics/antimycotics (all from Invitrogen), and the following angiogenic supplements: 75 μg/mL endothelial cell growth supplement (ECGS), 50 μg/mL heparin, 1 μg/mL hydrocortisone (all from Sigma-Aldrich), 50 ng/mL recombinant human (rh) $VEGF_{165}$, 25 ng/mL rhFGF-2, and 10 ng/mL rhEGF (all from Invitrogen) (referred as angiogenic medium). The angiogenic medium was changed every 2 days for a total period of 28 days. Endothelial transdifferentiation was evaluated by morphological characteristics, in vitro capillary-like network formation assay, real-time polymerase chain reaction (PCR), flow cytometric, and western blot analyses to determine the expression of a panel of angiogenic markers more analytically as follows:

In vitro capillary-like network formation assay. The potential of SCAP to develop capillary-like structures was evaluated on collagen gel matrices. Briefly, 500 μL of collagen I solution (rat tail collagen I; BD Biosciences) prepared according to the manufacturer's instructions was added to each well of a six-well plate and allowed to gel under alkaline pH for 1 h at 37°C. SCAP exposed to angiogenic medium for 14 days were trypsinized and 5×10^4 cells were resuspended in angiogenic medium and plated onto the gel matrix. After 24 h, cells were visualized using a phase-contrast microscope (Zeiss Axiovert 40; Carl Zeiss Micro Imaging, GmbH) for their ability to form capillary-like structures. SCAP expanded for the same period of time with CCM were used as negative control.

Quantitative real-time PCR and semiquantitative reverse transcription-PCR. Total mRNA was isolated using the Nucleospin RNA isolation kit (Macherey Nagel) and reverse transcribed (1 μg/sample) using the superscript first-strand synthesis kit (Invitrogen), according to the manufacturer's instructions. Reactions were performed using SYBR-Select PCR Master Mix (Applied Biosystems) in a Step One Plus thermal cycler (Applied Biosystems). All reactions started with two initial incubation steps at 50°C for 2 min for uracil-N-glycosylase activation and at 95°C for 2 min for activation of the AmpliTaq DNA polymerase and were followed by 40 cycles of PCR, comprising denaturation for 15 s at 95°C and annealing/extension for 1 min at 60°C. Primers were designed for the following genes: *PECAM1*, *VEGFA*, *VEGFR1*, *VEGFR2*, *ANGPT1*, *ANGPT2*, *TIE1*, *TIE2*, hypoxia-inducible transcription factor *HIF1A*, *HIF2A*, and *HIF1B* (Table 1). A standard melting curve was used to

Table 1. Primers Designed for the Real-time PCR and SemiQuantitative RT-PCR (vWF, CDH5) Analyses of Several Angiogenesis-Related Genes and the Respective Amplicon Sizes of the PCR Products

Gene symbol	*Forward (5′-3′)*	*Reverse (5′-3′)*	*Amplicon size (bp)*
PECAM1	GTCAAGCCTCAGCACCAGAT	GCTGGTACTCTGCAGTGGTT	175
VEGFA	AGGAGGGCAGAATCATCACG	CCAGGGTCTCGATTGGATGG	80
VEGFR1	TTAGGACCAGGAAGCAGCAC	GAGCCAGAAGAGAGTCGCAG	198
VEGFR2	CGGTCAACAAAGTCGGGAGA	CAGTGCACCACAAAGACACG	123
ANGPT1 (Ang-1)	ATGGGGGAGGTTGGACTGTA	TGCCTCTGACTGGTAATGGC	151
ANGPT2 (Ang-2)	TTGGCCGCAGCCTATAACAA	ACAGCATTGGACACGTAGGG	152
TIE1 (Tie-1)	CCATCCTGGCTGCCCTTTTA	CGGGTAAGTGTCAAGGTCCC	136
TIE2 (Tie-2)	AGGACGTGTGAGAAGGCTTG	GTGGCACAGGAACACCCATA	128
HIF1A	GCTTTAACTTTGCTGGCCCC	TTTTCGTTGGGTGAGGGGAG	140
HIF2A (EPAS1)	GCGACCATGAGGAGATTCGT	GACCGTGCACTTCATCCTCA	116
HIF1B (ARNT)	ACTACTGCCAACCCCGAAAT	CTCTGGACAATGGCTCCTCC	107
VWF	GTGAAGTAGCCCGCCTCCGC	GGTGCACACATCGCAGCCC	437
CDH5	GCCAAGCCCTACCAGCCC	CCGCCCTCCTCGTCGTAG	512
B2M	TGTCTTTCAGCAAGGACTGGT	ACATGTCTCGATCCCACTTAAC	138
SDHA (SDH)	GCATGCCAGGGAAGACTACA	GCCAACGTCCACATAGGACA	127

check the quality of amplification and specificity. The results were adjusted by amplification efficiency (LinRegPCR) and were normalized to the two most stable housekeeping genes evaluated by geNorm (succinate dehydrogenase complex, subunit A, flavoprotein-SDH-A, and beta-2-microglobulin-B2M).

Moreover, since no baseline expression of VE-cadherin (CDH5) and von Willebrand factor (VWF) could be detected in undifferentiated SCAP cultures to be used for real-time PCR data normalization, semiquantitative reverse transcription-PCR was used to show increase of expression of these markers in the course of their endothelial transdifferentiation. For RT-PCRs, the SuperScript One-Step reverse transcription-PCR System Polymerase kit (Invitrogen) was used. Briefly, 1 μg of total RNA was diluted in a PCR reaction of 1× PCR buffer containing 1.2 mM $MgCl_2$, 0.2 mM of each dNTP, a mixture of Superscript II Reverse Transcriptase/Platinum Taq DNA polymerase, and 10 pmol of each human-specific primer sets for CDH5 and vWF (Table 1). The reactions were performed in a PCR thermal cycler (AB 2720; Applied Biosystems) at 50°C for 30 min for cDNA synthesis, 94°C for 2 min for one cycle, and then at 94°C/(45 s), 60°C/(60 s), and 72°C/(60 s) for 35 cycles, with a final 10-min extension at 72°C. RT-PCR products were analyzed by 1.5% w/v agarose gel electrophoresis and visualized by ethidium bromide staining. RNA isolated from human umbilical vein endothelial cells (HUVECs; Lonza) was used as positive control for all reactions.

Flow cytometry. Flow cytometry was performed to evaluate the percentage of cell population expressing the endothelial differentiation marker, CD31/PECAM-1, and the endothelial stem cell marker, CD105/endoglin, during the course of endothelial transdifferentiation. SCAP were double stained with the fluorochrome-conjugated mouse anti-human antibodies, CD105-FITC and CD31-APC-Cy7 (both from Biolegend), as already described and analyzed with a BD LSR II Flow Cytometer.

Western blot analysis. Total protein was isolated from SCAP exposed to angiogenic medium for 0, 3, 7, 14, and 21 days. Briefly, cells were washed in ice-cold PBS and were lysed on ice using a buffer consisting of 50 mM tris-HCl (pH = 7.5), 150 mM NaCl, 0.5% v/v sodium deoxycholate, 5% NP-40, 1 mM phenyl methyl sulfonyl fluoride, 0.1 mM dithiothreitol, 10 μM aprotinin, and 10 μM leupeptin to yield total cellular protein extracts after centrifugation at 10,000 rpm for 10 min. Protein concentrations were quantified using a BCA Protein Assay Kit (Sigma-Aldrich) according to the manufacturer's instructions and measured spectrophotometrically at 562 nm by a microplate reader (Epock; Biotek, Biotek Instruments, Inc.). An equal amount of protein from each sample (40 μg for PECAM-1 and 5 μg for GAPDH) was separated on a 10% and 12% (respectively) sodium dodecyl sulfate–polyacrylamide gel by electrophoresis and then transferred onto a polyvinylidene fluoride (Millipore) membrane at 240 mA for 1.5 h. After blocking in 5% nonfat dry milk (Blotto; Santa Cruz Biotech) in PBS, the membranes were incubated overnight at 4°C with the following primary antibodies diluted in the same blocking buffer: monoclonal rabbit anti-human CD31 (1:1,000; Abcam) and monoclonal mouse anti-human GAPDH (1:2,000; Acris) used as loading control. The membranes were then washed with PBS containing Tween 20 and incubated with secondary goat anti-mouse or anti-rabbit-conjugated horseradish peroxidase (HRP) antibodies (1:10,000; Millipore) for 1 h at room temperature, developed with an enhanced chemiluminescence (ECL) substrate (Novex, Life technologies) and visualized using an ECL imaging system (MicroChemi; DNR Bio-Imaging Systems Ltd.).

Evaluation of the endothelial transdifferentiation potential of SCAP occurring in stress microenvironments

SCAP were first expanded with normal CCM until reaching 70%–80% confluency. Subsequently, the medium was changed with media with or without serum and/or glucose, and the cells were incubated for 72 h under either normoxic or hypoxic conditions. For induction of OD, a 93:5:2 mixture of $N_2/CO_2/O_2$ in a hypoxic chamber was used. For induction of SD, a 2% FBS concentration was selected to avoid protein aggregation possible at lower serum concentrations. For induction of GD, a glucose-free Dulbecco's modified Eagle's medium (Invitrogen) was used. By using these stress factors separately or in combination, six experimental groups (G) were formed as follows:

G1: Cells exposed to CCM (DMEM containing 1 g/L glucose, 15% FBS, and 1% antibiotics/antimycotics) were incubated under normoxic conditions [CCM (N)]

G2: Cells exposed to CCM as described above were incubated under hypoxic conditions [CCM (H + G)]

G3: Cells exposed to CCM without glucose (DMEM without glucose, with 15% FBS, and 1% antibiotics/antimycotics) were incubated under hypoxic conditions [CCM (H–G)]

G4: Cells exposed to medium containing 2% FBS [DMEM containing 1 g/L glucose, 2% FBS, and 1% antibiotics/antimycotics = serum deprivation medium (SDM)] were incubated under normoxic conditions [SDM (N)]

G5: Cells exposed to SDM as described above were incubated under hypoxic conditions [SDM (H + G)]

G6: Cells exposed to SDM without glucose (DMEM without glucose, with 2% FBS, and 1% antibiotics/antimycotics) were incubated under hypoxic conditions [SDM (H–G)]

This experimental design allowed studying the impact of each stress-induced factor (ie, SD, OD, and GD) separately or in combination on the angiogenic potential of SCAP. At the end of the incubation period, total RNA was collected from each experimental group and processed for real-time PCR analysis, as described above. Additionally, culture supernatant was collected from each group of cultured cells for identification of secreted soluble angiogenic factors (see below).

Exposure of SCAP to various stress microenvironments and analysis of the angiogenic properties of their secretome

SCAP were cultured under the stress conditions described above (G1–6). Conditioned media (CM) collected from these cultures were centrifuged at 200 *g* for 5 min to remove any cell debris, filtered through a 0.2-μm filter, and stored at −80°C until used. CCM (15% FBS) and SDM (2% FBS) processed similarly [nonconditioned media (NCM)] served as controls. CMs and NCMs were analyzed for identification of angiogenic factors using a proteome profiler array and enzyme-linked immunosorbent (ELISA) colorimetric assays. ELISA was performed for both CCM-based CMs (G1–3) and SDM-based CMs (G4–6). The proteome profiler array was performed only for the SDM-based CMs (G4–6)

and the respective control medium (SDM 2% FBS) to avoid the data being obscured on the membranes by the high serum concentration of the CCM analytically as follows:

Antibody array for detection of pro- and antiangiogenic factors in CMs. To identify angiogenic factors in SDM-based CMs (G4–6), an antibody array (Proteome ProfilerTM Human Angiogenesis Antibody Array; R&D Systems) was performed according to the manufacturer's instructions. Briefly, the array membranes were incubated with a blocking buffer for 1 h at room temperature. While the membranes were blocking, 700 μL of each CM was incubated with detection antibodies for 1 h at room temperature. Next, sample/antibody mixtures were added to the membranes and incubated overnight at 4°C on a rocking platform. Following several wash steps, the membranes were incubated with horseradish peroxidase-conjugated streptavidin for 30 min. Next, the membranes were washed again and exposed to a chemiluminescent reagent mix for 1 min at room temperature. Light signals were detected by exposing the membranes to an X-ray film (Fuji) for 5 min. The detected spots were quantified using the ImageJ Software and the dot blot macromodule [27].

Enzyme-linked immunosorbent assays. The protein levels of key angiogenic factors (VEGF, FGF-2) as well as of TGF-β1, a factor known to enhance EC viability and migration [28], were measured in collected CMs (G1–6) to quantitatively validate the results of the proteome profiler array. For this purpose, sandwich colorimetric ELISA kits were obtained from R&D Systems and assays were performed

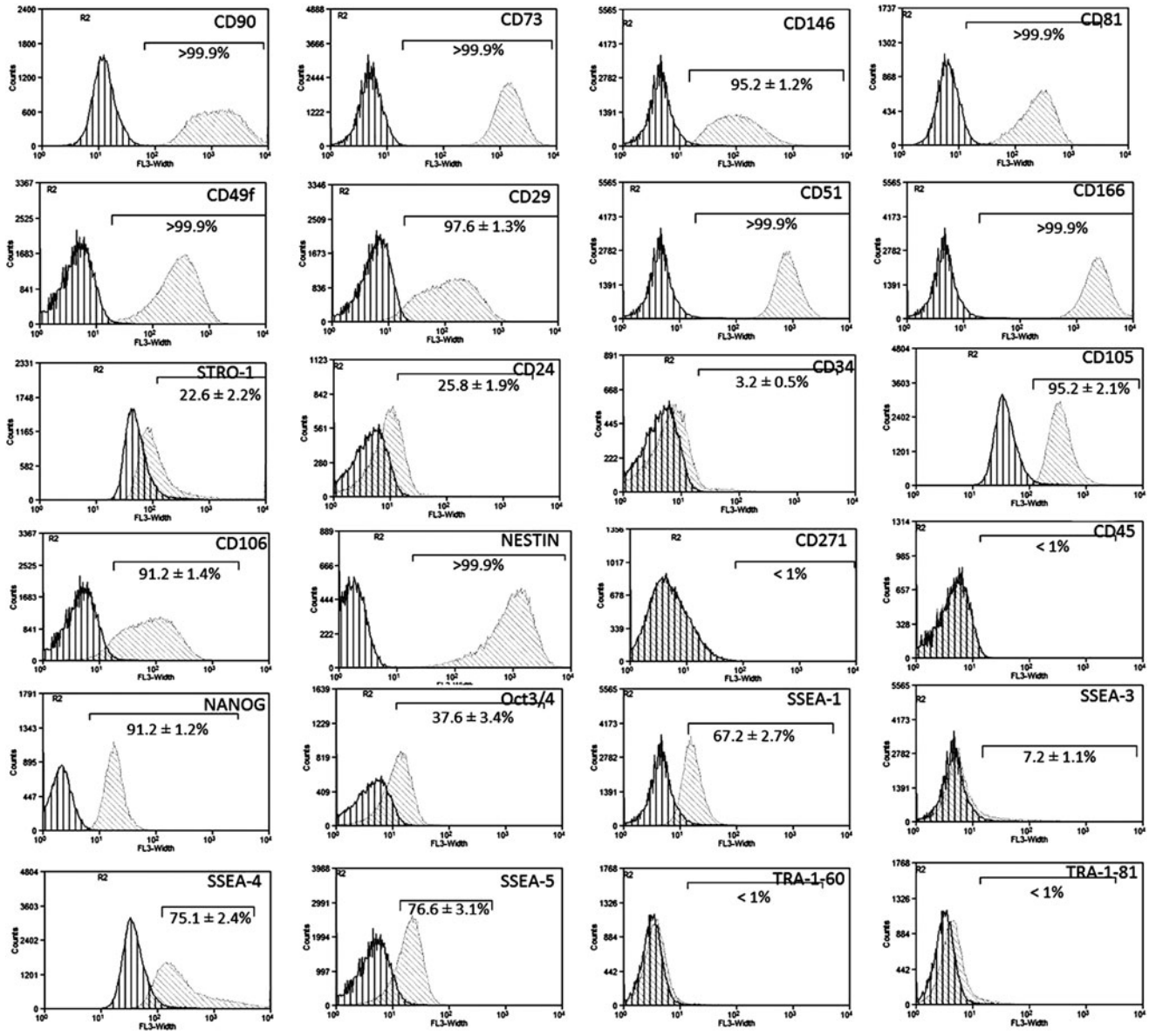

FIG. 1. Immunophenotypic characterization of stem cells from the apical papilla (SCAP) by flow cytometry. Representative single-parameter diagrams showing the expression of mesenchymal (CD90/Thy-1, CD73, CD146/MUC18, CD81/TAPA-1, CD49f/a6-integrin, CD29/b1-integrin, CD51/av-integrin, CD166/ALCAM, STRO-1, CD24, CD34), endothelial (CD105/endoglin, CD106/VCAM), neural (CD271/NGFR, nestin), hematopoietic (CD45), and embryonic (Nanog, Oct3/4, SSEA-1, -3, -4, -5, TRA-1-60, and TRA-1-81) SC markers (*dark gray line/left*: isotype control, *light gray line/right*: marker of interest). Results are expressed as means ± standard deviations of three independent experiments.

following the manufacturer's instructions. Baseline values for VEGF, FGF-2, and TGF-β1 contained in nonconditioned SDM (2% FBS) and CCM (15% FBS) were subtracted from the values measured in respective CMs (G1–6).

Angiogenic impact of SCAP secretome on HUVECs

CMs collected from SCAP cultured under the abovementioned stressful microenvironments were compared for their potential to promote migration and formation of endothelial tubular structures by HUVECs as follows:

In vitro transwell migration assay-blocking experiments. This assay is based on the potential of cells to migrate through a porous membrane as a response to a chemical attractant. HUVECs were first cultured on collagen I-coated flasks in M199 medium, supplemented with 20% FBS, 1% antibiotics/antimycotics, 75 μg/mL ECGS, and 50 μg/mL heparin. After reaching 80% confluency, HUVECs were serum starved in M199 medium containing 2% FBS for 12 h and then transferred at 10^5/100 μL density onto collagen I-coated (10 μg/cm^2) polyester (PET) transwell inserts of 24-well plates with a 8-μm membrane pore size (Corning, Life Sciences, Ltd.). The cells were seeded at the top of the membranes, and the six different CMs were added as chemoattractant in the lower chamber. SDM (2% FBS) and CCM (15% FBS) NCM were used as negative and positive controls, respectively.

After 6 h, the medium was aspirated and the upper surface of each membrane was gently swabbed to remove any nonmigrated cells. Membranes were fixed with 10% neutral buffered formalin and stained with crystal violet solution (0.5%) (Sigma-Aldrich). Photographs of the stained cells were taken from five random fields of view (×10) for each membrane under an inverted microscope (Zeiss Axiovert 40) equipped with a digital camera. Quantification was performed by means of Carl Zeiss Axiovision 4.6 Software. Values were expressed as migration percentages (%) by dividing the average of cells counted in all optical fields by the area of the microscope viewing field, and then multiplying this number by the entire area of the transwell insert to obtain the total number of migrated cells. The percentage of migration was then calculated by the ratio of migrated cells to the initial number of seeded cells × 100%.

For the in vitro blocking experiments, VEGF and TGF-β1 were blocked in all CMs with the use of neutralizing Abs (mouse anti-human VEGF, clone 6D3; NOVUS, and mouse anti-human anti-TGF-β1, clone TB21; Acris) at a concentration of 5 μg/mL for 30 min at 4°C. CM was also incubated under the same conditions with an irrelevant isotype control Ab (IgG1) (Sigma-Aldrich).

In vitro capillary-like network formation assay-blocking experiments. HUVECs were cultured on collagen gel matrices, as already described for SCAP. HUVECs were first expanded to 80% confluency and then switched to low FBS (SDM, 2% FBS) for 12 h. Next, HUVECs were seeded at 10^5 cells/well onto the gel matrices and incubated with each one of the six different CMs, as well as with SDM and CCM NCM serving as negative and positive controls, respectively. After 24 h, HUVECs were stained with 2 μM calcein acetomethoxy derivative of calcein (calcein AM) (Invitrogen) for 30 min at room temperature and then examined under a fluorescent microscope (Zeiss Axiovert 40) equipped with a digital camera. Number of master junctions, number of master segments, and total master segment length per optical field were quantified using the ImageJ Software [27] and the angiogenesis analyzer macromodule on images at 10× magnification ($n = 5$). Additional experiments were performed after blocking the CMs with the same neutralizing Abs, as described for the in vitro transwell migration assay.

Statistics

All experiments were run in duplicate samples and repeated at least thrice. Statistical analysis of the data was performed by one-way ANOVA with Bonferroni's post hoc test and by a two-tailed *t*-test using Prism 6.0 Software (GraphPad) ($^*P < 0.05$ and $^{**}P < 0.01$). Data are expressed as mean ± standard deviation.

Results

Immunophenotypic profiles of SCAP

SCAP cultures were highly positive (>95% of the population) for MSC markers, including CD90/Thy-1, CD73, CD146/MUC18, CD81/TAPA and the cell adhesion molecules (CAMs) CD49f/a6-integrin, CD29/b1-integrin, CD51/av-integrin, and CD166/ALCAM. Lower expression was observed for the MSC markers, STRO-1 (22.6% ± 2.2%), CD24 (25.8% ± 1.9%), and CD34 (3.2% ± 0.5%). The endothelial SC markers, CD105 (95.2% ± 2.1%) and CD106 (91.2% ± 1.4%), were also highly expressed. Interestingly, high expression was

FIG. 2. **(A)** Representative phase-contrast microphotographs of SCAP cultures. **(a)** In confluency before exposure to angiogenic medium. **(b)** Fourteen days after seeding on collagen I-coated plates and exposure to angiogenic medium, showing the development of a capillary-like network over the dense monolayer, and **(c)** 14 days after exposure to angiogenic medium, followed by trypsinization and reseeding at very low density (5×10^4 cells/well of six-well plates) on thick (3 mm) and dense (~1 mg/mL) collagen gel matrices. SCAP formed typical capillary-like structures, indicative of an endothelial cell (EC)-phenotype. **(B)** Real-time polymerase chain reaction (PCR) analysis of the expression of several angiogenesis-related molecules, including PECAM-1, vascular endothelial growth factor (VEGF), VEGFR-1, VEGFR-2, angiopoietin-1 (Ang-1), Ang-2, Tie-1, and Tie-2, and semiquantitative reverse transcription-PCR analysis of von Willebrand factor (vWF) and VE-cadherin expression in SCAP cultures exposed to angiogenic medium for up to 28 days. Human umbilical vein endothelial cells (HUVECs) were used as positive controls and beta-2-microglobulin (B2M) and SDHA as housekeeping genes for this assay. Real-time PCR values are means ± standard deviations of three independent experiments in duplicates ($^*P < 0.05$, $^{**}P < 0.01$ compared with control untreated cultures). **(C)** Representative single-parameter flow cytometry diagrams showing the percentage of cell population positive for CD31 and CD105 during the course of endothelial transdifferentiation of SCAP. Cells were examined after 3, 7, 14 and 21 days of exposure to angiogenic medium (D3 to D21). Results are expressed as means ± standard deviations of three independent experiments ($^*P < 0.05$, $^{**}P < 0.01$ compared with control untreated cultures). **(D)** Representative western blots showing obvious increase of PECAM-1 (CD31) protein expression 14 and 21 days after exposure to angiogenic medium. GAPDH was used as loading control protein.

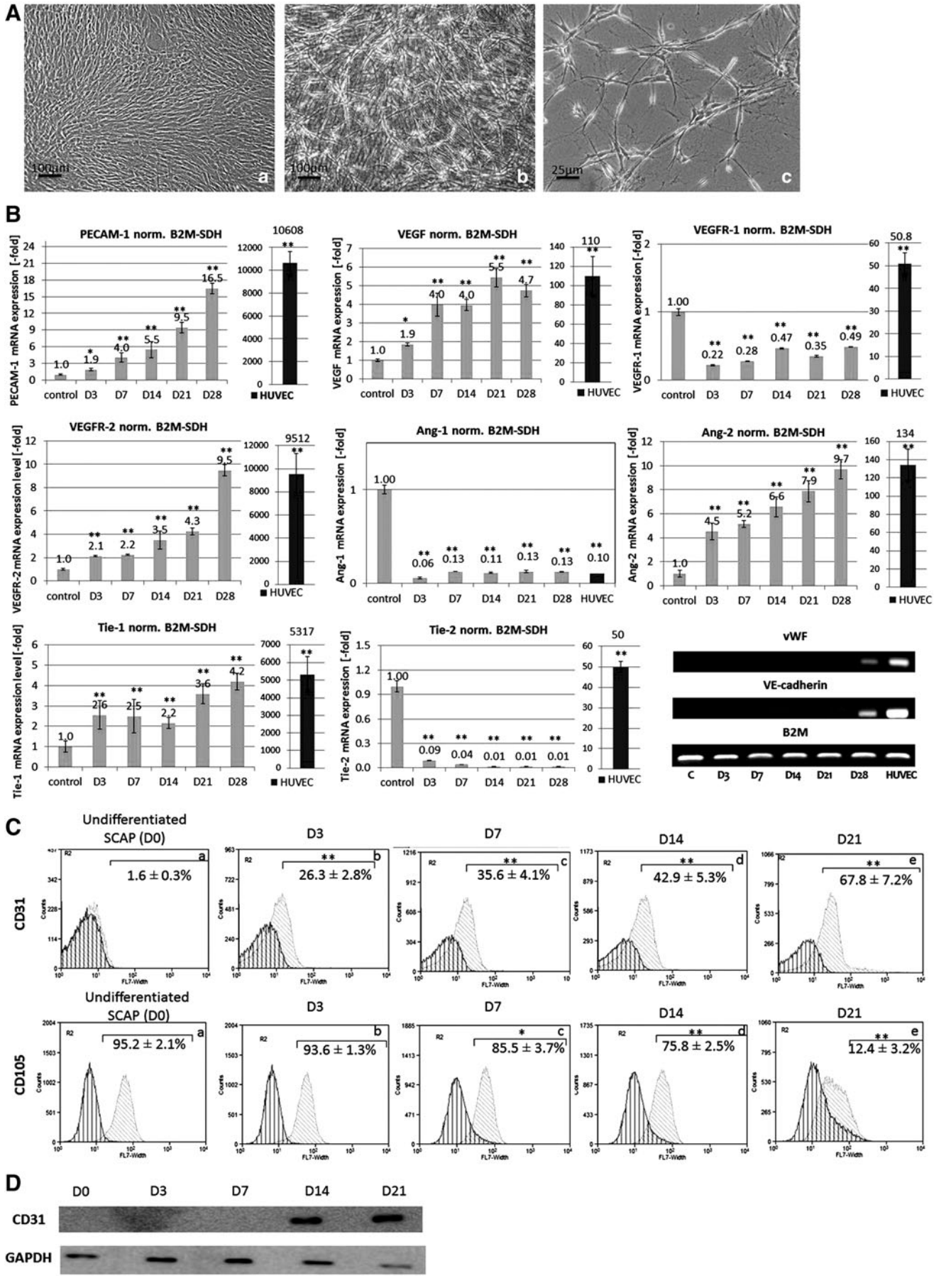
A
100µm
a
100µm
b
25µm
c
B
PECAM-1 norm. B2M-SDH
PECAM-1 mRNA expression [-fold]
10608
VEGF norm. B2M-SDH
VEGF mRNA expression [-fold]
110
VEGFR-1 norm. B2M-SDH
VEGFR-1 mRNA expression [-fold]
50.8
VEGFR-2 norm. B2M-SDH
VEGFR-2 mRNA expression level [-fold]
9512
Ang-1 norm. B2M-SDH
Ang-1 mRNA expression [-fold]
Ang-2 norm. B2M-SDH
Ang-2 mRNA expression [-fold]
134
Tie-1 norm. B2M-SDH
Tie-1 mRNA expression level [-fold]
5317
Tie-2 norm. B2M-SDH
Tie-2 mRNA expression [-fold]
50
control D3 D7 D14 D21 D28
HUVEC
vWF
VE-cadherin
B2M
C D3 D7 D14 D21 HUVEC
C
Undifferentiated SCAP (D0)
D3
D7
D14
D21
CD31
1.6 ± 0.3%
26.3 ± 2.8%
35.6 ± 4.1%
42.9 ± 5.3%
67.8 ± 7.2%
CD105
95.2 ± 2.1%
93.6 ± 1.3%
85.5 ± 3.7%
75.8 ± 2.5%
12.4 ± 3.2%
FL7-Width
Counts
D
D0 D3 D7 D14 D21
CD31
GAPDH

also recorded for the neural SC marker Nestin (>99%), but not for CD271/NGFR (<1%). The hematopoietic SC marker CD45 was not expressed (<1%). Finally, SCAP showed a differential expression of various embryonic SC markers as follows: Nanog (91.2% ± 1.2%), Oct3/4 (37.6% ± 3.4%), SSEA-1 (67.2% ± 2.7%), SSEA-3 (7.2% ± 1.1%), SSEA-4 (75.1% ± 2.4%), SSEA-5 (76.6% ± 3.1%), TRA-1-60 (<1%), and TRA-1-81 (<1%) (Fig. 1).

Time course endothelial transdifferentiation of SCAP into ECs

The first part of this study focused on the endothelial transdifferentiation potential of SCAP under various microenvironmental conditions. Exposure of SCAP to angiogenic medium for 28 days was associated with morphological changes toward an endothelial-like phenotype, acquisition of a capillary-like-forming potential, and an increase in expression of several angiogenesis-related genes involved in both VEGF/VEGFR and angiopoietin/Tie angiogenesis systems (see as follows).

Induction of morphological changes and capillary-like tubule formation after exposure to the angiogenic medium. SCAP seeded on collagen I-coated plates [Fig. 2A(a)] and exposed to the angiogenic medium formed, during the time course of their endothelial transdifferentiation, a multilayered structure, with elongated cells forming capillary-like structures over the dense monolayer [Fig. 2A (b)]. Trypsinization and reseeding of the cells at low density on thick (3 mm) and dense collagen gel matrices resulted in sprouting derived from single cells (single-cell nodes) and subsequent development of capillary-like structures to finally shape an extensive lattice [Fig. 2A (c)].

Time course gene expression of angiogenesis-related markers. Continuous exposure of SCAP to the angiogenic medium led to a time-dependent induction of angiogenesis-related molecules, including PECAM-1 (up to 16.5 ± 1.1-fold), VEGF (up to 5.5 ± 0.5-fold), vWF, and CDH5 (semiquantitative data) (Fig. 2B). This was followed by significant upregulation of the expression of the receptor VEGFR-2 (9.5 ± 0.5-fold) and parallel downregulation of VEGFR-1. A similar effect was observed at the transcriptional level for Ang-2 and Ang-1 (two key players of the angiopoietin/Tie system), which were activated up to 9.7 ± 0.8-fold and markedly repressed, respectively (Fig. 2B). Interestingly, the expression of the Ang-1/Ang-2 receptor Tie-2 was robustly downregulated, whereas the expression of the receptor Tie-1 significantly increased during SCAP endothelial transdifferentiation.

It should also be noted that despite the obvious increase in expression of angiogenesis-related molecules, the mRNA steady-state level of these markers was kept significantly lower than that seen in mature ECs (HUVEC) even after 28 days of continuous exposure to angiogenic medium (Fig. 2B). This suggests acquisition of a proendothelial phenotype by SCAP (ie, vascular endothelial precursors) compared with terminally differentiated ECs (HUVEC). Flow cytometric analysis confirmed that there was a time-dependent increase of the proportion of the cell population expressing the PECAM-1 (CD31) from 1.6% ± 0.3% in undifferentiated SCAP cultures (control) up to 67.8% ± 7.2% 21 days after exposure to angiogenic medium, while the proportion of cells exhibiting the endothelial stem cell marker, CD105 (>95%), progressively decreased to 12.4% ± 3.2% after 21 days of exposure to the angiogenic medium (Fig. 2C). Finally, western blot analysis confirmed obvious upregulation of PECAM-1 (CD31) protein expression after 14 and 21 days of exposure to angiogenic medium, although this method was less sensitive in detecting early PECAM-1 expression increase compared with the flow cytometric analysis (Fig. 2D).

Endothelial transdifferentiation potential of SCAP in various stress microenvironments

Exposure of SCAP to stress microenvironments (ie, SD, OD, and GD either individually or in combination) for 72 h elicited a proangiogenesis program at various degrees in these cells. One-way analysis of variance and Bonferroni's post hoc test showed that the potency of angiogenic induction increased as follows: N ≤ H+G < H−G for the expression of PECAM-1, VEGF, VEGFR-2, Tie-1, and Tie-2 and N > H+G < H−G for Ang-2. Moreover, under the same conditions of oxygen and/or GD, a lower serum concentration (SDM) was more effective in inducing a proangiogenesis program compared with high serum concentration (CCM), that is, CCM < SDM for several angiogenic factors, as shown in Fig. 3A. It was noteworthy that when SCAP were exposed for 3 days to low serum medium (SDM) under

FIG. 3. **(A)** Real-time PCR analysis of the expression of angiogenesis-related molecules, including PECAM-1, VEGF, VEGFR-1, VEGFR-2, Ang-1, Ang-2, Tie-1, and Tie-2, and for the hypoxia-inducible transcription factor (HIF)-1A, HIF-2A, and HIF-1B subunits after exposure of SCAP for 72 h to the following microenvironments: group 1 [complete culture medium, CCM (N)], SCAP exposed to CCM [15% fetal bovine serum (FBS) + 1 g/L glucose] in normoxia; group 2 [CCM (H+G)], SCAP exposed to CCM (15% FBS + 1 g/L glucose) in 2% hypoxia; group 3 [CCM (H−G)], SCAP exposed to CCM (15% FBS without glucose) in 2% hypoxia; group 4 [serum deprivation medium, SDM (N)], SCAP exposed to SDM (2% FBS + 1 g/L glucose) in normoxia; group 5 [SDM (H+G)], SCAP exposed to SDM (2% FBS + 1 g/L glucose) in 2% hypoxia; and group 6 [SDM (H−G)], SCAP exposed to SDM (2% FBS without glucose) in 2% hypoxia. Values are means ± standard deviations of three independent experiments in duplicates. *Black asterisks* indicate statistically significant differences between N, H+G, and H−G conditions within the same serum concentration group (CCM or SDM), and *gray asterisks* (in the rectangular frame) indicate statistically significant differences between CCM and SDM for similar oxygen/glucose conditions [ie, CCM (N) vs. SDM (N), CCM (H+G) vs. SDM (H+G), CCM (H−G) vs. SDM (H−G)] (*$P < 0.05$, **$P < 0.01$). **(B)** Representative phase-contrast microphotographs of SCAP cultures exposed to various stress microenvironments **(a–f)**. No morphological changes could be observed in cultures exposed to CCM (N), CCM (H+G), SDM (N), and SDM (H+G) (groups 1, 2, 4, and 5), whereas, in cultures exposed to hypoxia in the absence of glucose (H−G) under both CCM and SDM conditions (groups 3 and 6), monolayers acquired a typical lumen-like appearance (scale bars 100 μm). **(g)** Graphic showing that SCAP retained high levels of cell viability after exposure for 72 h to all stress microenvironments, as shown by trypan blue exclusion. No statistically significant differences were observed compared with cells grown under CCM (N) (control).

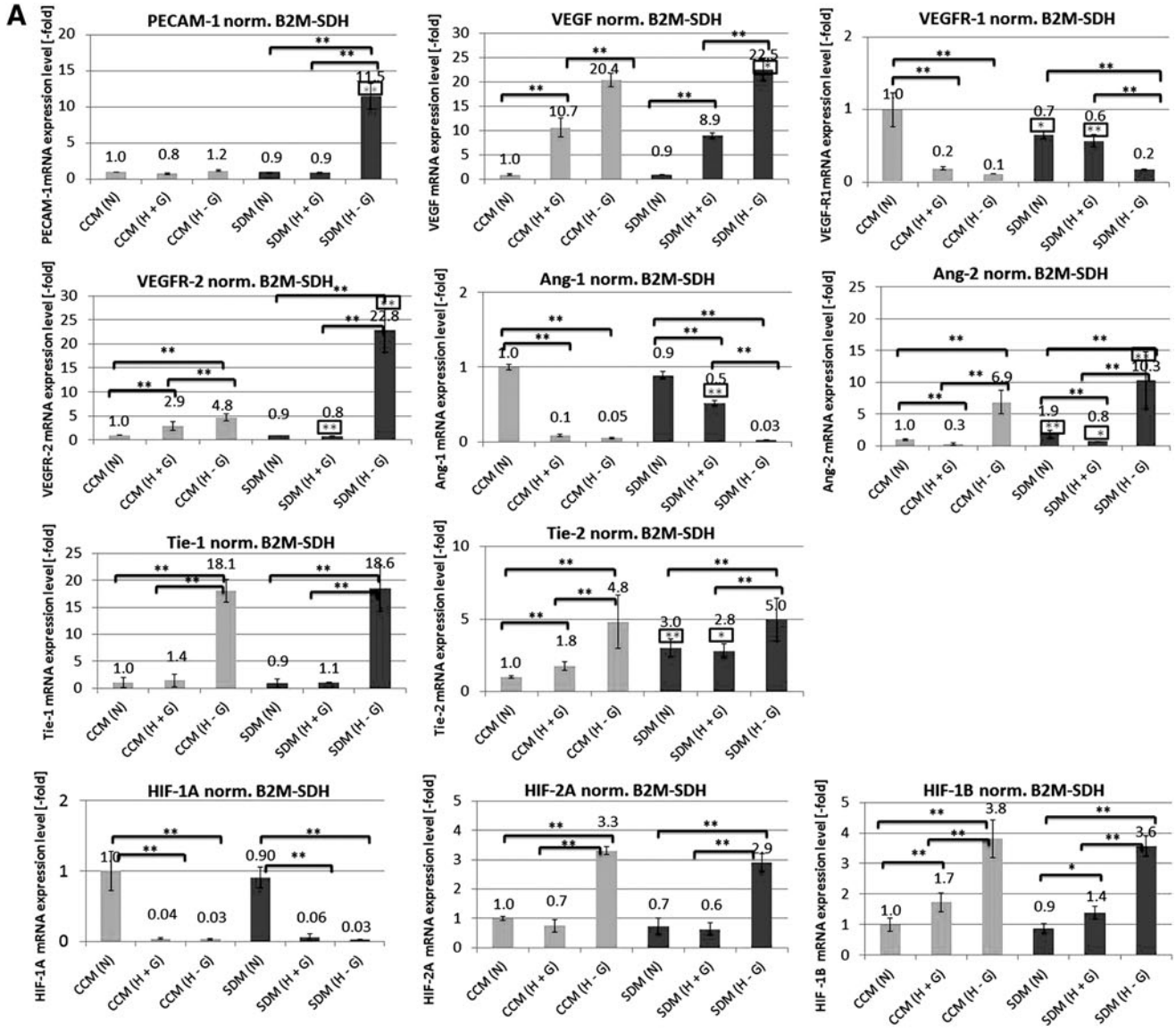
A
PECAM-1 norm. B2M-SDH
PECAM-1mRNA expression level [-fold]
VEGF norm. B2M-SDH
VEGF mRNA expression level [-fold]
VEGFR-1 norm. B2M-SDH
VEGFR-1mRNA expression level [-fold]
VEGFR-2 norm. B2M-SDH
VEGFR-2 mRNA expression level [-fold]
Ang-1 norm. B2M-SDH
Ang-1 mRNA expression level [-fold]
Ang-2 norm. B2M-SDH
Ang-2 mRNA expression level [-fold]
Tie-1 norm. B2M-SDH
Tie-1 mRNA expression level [-fold]
Tie-2 norm. B2M-SDH
Tie-2 mRNA expression level [-fold]
HIF-1A norm. B2M-SDH
HIF-1A mRNA expression level [-fold]
HIF-2A norm. B2M-SDH
HIF-2A mRNA expression level [-fold]
HIF-1B norm. B2M-SDH
HIF -1B mRNA expression level [-fold]
CCM (N)
CCM (H + G)
CCM (H - G)
SDM (N)
SDM (H + G)
SDM (H - G)

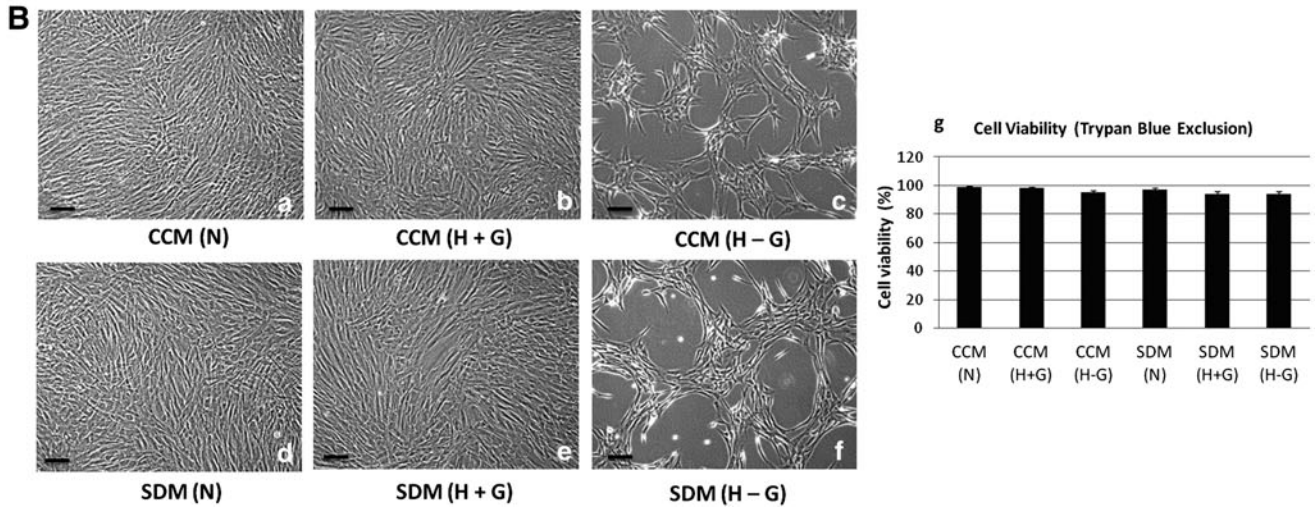
B
a
b
c
d
e
f
CCM (N)
CCM (H + G)
CCM (H – G)
SDM (N)
SDM (H + G)
SDM (H – G)
g
Cell Viability (Trypan Blue Exclusion)
Cell viability (%)
CCM (N)
CCM (H+G)
CCM (H-G)
SDM (N)
SDM (H+G)
SDM (H-G)

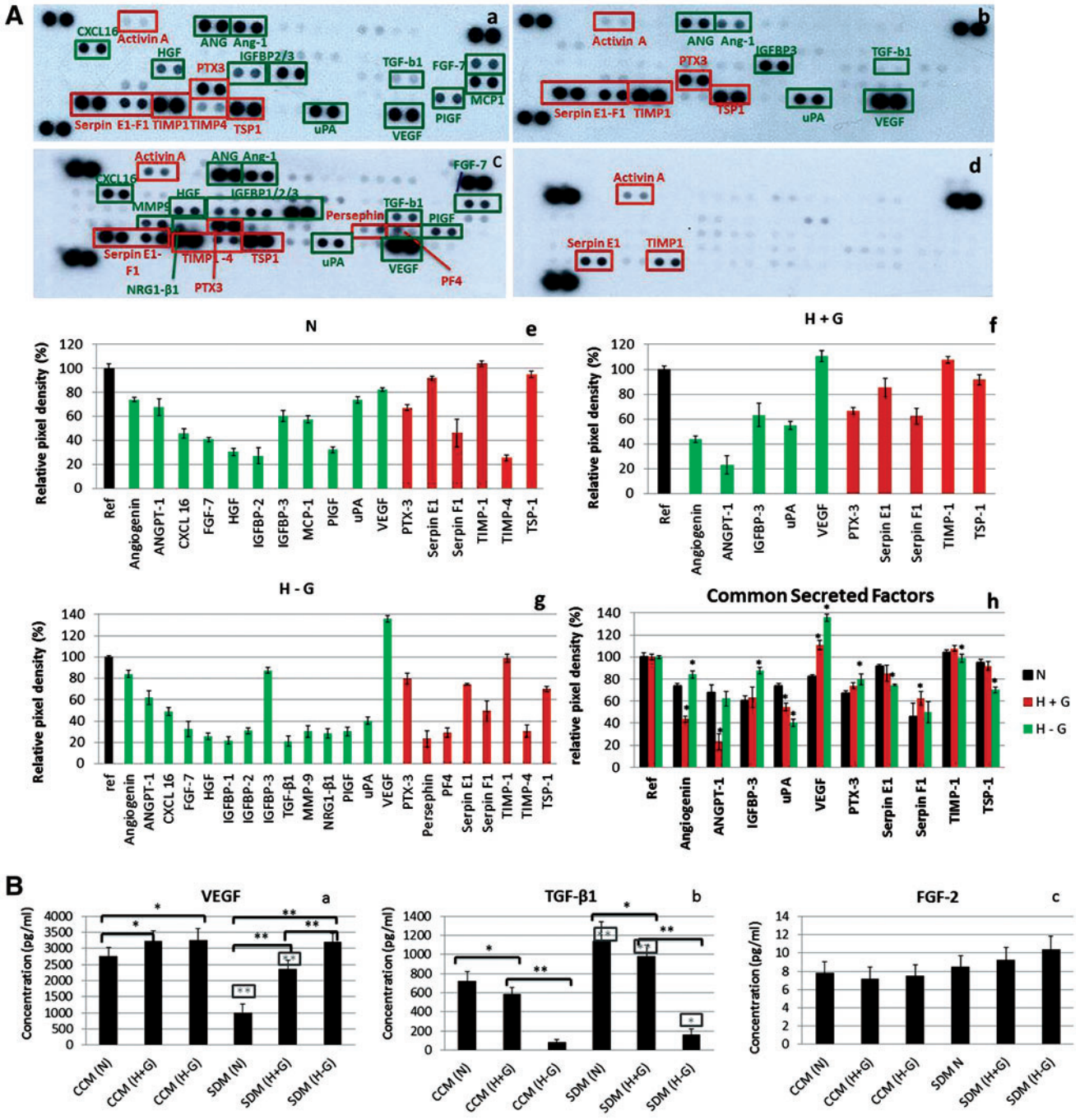

FIG. 4. **(A)** Representative proteome profiler arrays, showing the presence of pro- (marked in *green*) and antiangiogenic (marked in *red*) factors in secretomes collected under **(a)** SDM (N), **(b)** SDM (H+G), **(c)** SDM (H–G), and **(d)** negative control (plain, nonconditioned SDM containing 2% FBS). Graphics **(e–h)** show the relative expression levels of angiogenic factors in each secretome as well as of the common secreted factors in all three different secretomes. Values were normalized to the positive reference *dots* of each membrane and are expressed as means ± standard deviations (*asterisks* indicate statistically significant differences of secreted factors under H+G and H–G conditions compared with N, $*P < 0.05$, $**P < 0.01$). **(B)** Enzyme-linked immunosorbent assays (ELISA) for quantification of **(a)** vascular endothelial growth factor (VEGF), **(b)** transforming growth factor beta 1 (TGF-β1), and **(c)** fibroblast growth factor-2 (FGF-2) concentrations (pg/mL) in SCAP secretomes collected under different stress conditions (groups 1–6). Baseline VEGF, TGF-β1, and FGF-2 values in respective nonconditioned media (CCM and SDM) were subtracted from values obtained in the assay to calculate the final growth factor concentrations in each secretome. Results are expressed as means ± standard deviations of three independent experiments in duplicates of secretomes collected from three different cell donors [*black asterisks* indicate statistically significant differences between N, H+G, and H–G conditions within the same serum concentration group (CCM or SDM), and *gray asterisks* (in the rectangular frame) indicate statistically significant differences between CCM and SDM for similar oxygen/glucose conditions, that is, CCM (N) vs. SDM (N), CCM (H+G) vs. SDM (H+G), and CCM (H–G) vs. SDM (H–G), $*P < 0.05$, $**P < 0.01$]. Color images available online at www.liebertpub.com/scd

conditions of oxygen and glucose deprivation [G6: SDM (H–G)], they acquired the same or even more pronounced angiogenic expression profiles (Fig. 3A) compared with those obtained after SCAP exposure for 28 days to the potent angiogenic medium (Fig. 2B). A similar effect—although to a lesser intensity compared with G6—was observed for SCAP incubated with CCM under oxygen/glucose deprivation conditions [G3: CCM (H–G)]. Under these conditions, a significant upregulation of VEGF, VEGFR-2, Ang-2, Tie-1, and Tie-2 and downregulation of VEGFR-1 and Ang-1 could be also observed.

Hypoxia with parallel GD was also associated with upregulation of the expression of HIF-2A and HIF-1B subunits, both under CCM and SDM conditions (G3 and 6, respectively) (Fig. 3A). In contrast, HIF-1A expression was significantly downregulated when hypoxia (in the presence or absence of glucose and/or serum, ie, G2, 3, 5, 6) was applied for 72 h. Significantly, no discrete morphological changes or reduction of cell viability (>95% as shown by trypan blue exclusion) could be observed in cultures exposed to CCM (N), CCM (H+G), SDM (N), and SDM (H+G) (G1, 2, 4, 5) [Fig. 3B (a, b, d, e)], whereas in cultures exposed to hypoxia in the absence of glucose (H–G) under both CCM and SDM conditions (G3 and 6, respectively), the appearance of the dense monolayer changed dramatically, acquiring a typical lumen-like appearance, indicative of an angiogenic phenotype [Fig. 3B (c, f)]. Cell morphology as well as viability [Fig. 3B (g)], however, were not affected in these groups, although cells ceased proliferating (microscopic observation). Overall, these data indicate a high adaptability of SCAP to adverse conditions of severe environmental stress.

Angiogenic properties of SCAP secretome in various stress microenvironments

The second part of the study aimed to identify angiogenesis-related molecules secreted into the CM from SCAP. A proteome profiler array was used to assess the relative protein level of 55 angiogenesis-related proteins. Interestingly, discrete secretome profiles were detected under N (17 detected factors), H+G (10 factors), and H–G (22 factors) conditions, with differential expression of several pro- (CXCL-16, HGF, PIGF, FGF-7, TGF-β1, MCP-1, VEGF, uPA, angiogenin, angiopoietins, MMP-9, IGFBP-1,-2,-3, NRG1-β1) and anti-angiogenic (TSP-1, PTX-3, TIMP-1, -4, serpin-E1 and F1, persephin, PF4) factors (marked as green and red, respectively) [Fig. 4A (a–d)]. Common secreted factors under all three conditions included angiogenin, Ang-1, IGFBP-3, uPA, VEGF (proangiogenic), and PTX-3, serpin-E1, -F1, TIMP-1, and TSP-1 (antiangiogenic). It has to be noted that several of these molecules have multiple functions not only being implicated in angiogenesis but also in tissue repair, inflammatory response, migration, etc. Additional factors were found to be differentially secreted under various conditions as follows: (1) normoxia (N): CXCL-16, IGFBP-2, HGF, PIGF, MCP-1, FGF-7, TIMP-4; (2) hypoxia in the presence of glucose (H+G): IGBP-3; and (3) hypoxia in the absence of glucose (H–G): CXCL-16, FGF-7, HGF, IGFBP-1, -2, -3, TGF-β1, MMP-9, pentraxin-3, NRG1-β1, persephin, PF4, PIGF, TIMP-4. The highest number of secreted factors was detected under H–G conditions.

Semiquantitative analysis of the relative amounts of secreted molecules revealed much higher amounts of proangiogenic factors (angiogenin, IGFBP-3, and VEGF) and lower amounts of antiangiogenic molecules (serpin-E1, TIMP-1, and TSP-1) released under H–G conditions compared with N conditions ($P < 0.05$) [Fig. 4A (e–h)]. In the case of H+G conditions, the main finding was a significantly higher secretion of VEGF ($P < 0.05$), but lower release of other proangiogenic factors, such as angiogenin and Ang-1 ($P < 0.05$) compared with N.

Since a much higher release of VEGF was a common finding under both hypoxic conditions (with or without the presence of glucose) compared with normoxia, the results of the proteome profiler array were further validated by an ELISA colorimetric assay [Fig. 4B (a)]. The results showed an increased secretion of VEGF in the following order: N < H+G < H–G both under CCM and SDM conditions (with CCM > SDM), therefore confirming the proteome profiler array data. ELISA was also performed for FGF-2—an important angiogenic factor that could not detected by the proteome profiler array—and for TGF-β1. The results showed a reverse order regarding release of TGF-β1 compared with VEGF, that is, N > H+G > H–G and CCM < SDM [Fig. 4B (b)], whereas the release of FGF-2 was overall very low (not exceeding 10 pg/mL, close to the detection limit of the FGF-2 ELISA kit), thereby confirming the results of the proteome profiler array regarding the absence of FGF-2 in SCAP secretome under all conditions studied [Fig. 4B (c)].

Role of SCAP secretome in modulating migration and vascular tubule formation potential of HUVEC

In this last part of the study, functional assays were performed to determine the potential of SCAP secretome-derived factors released under various stress conditions to induce migration and vascular tubule formation by HUVECs. In addition, blocking experiments were performed using neutralizing Abs for VEGF and TGF-β1 to confirm their effects, as justified below. Blocking of VEGF was selected because, apart from being a grave angiogenic factor, its secretion significantly increased under H+G and H–G compared with N conditions, while blocking of TGF-β1 was chosen due to its key biological role in inducing migration of various cell types, including ECs [28].

Results showed that SCAP secretome induced pronounced migration of HUVECs within 6 h (ranging between 56.5% and 92.1% in various experimental groups), which was at a statistically significantly lower [G1: CCM (N), G2: CCM (H+G), G4: SDM (N)], similar [G3: CCM (H–G), G5: SDM (H+G)], or higher [only for G6:SDM (H–G)] level than that induced by the chemoattractant medium (aMEM with 15% FBS) used as positive control (77.9% ± 10.9%). One-way analysis of variance and Bonferroni's post hoc test revealed statistically significant differences among groups ($P < 0.05$), with N < H+G < H–G and CCM < SDM for the same oxygen/glucose conditions [ie, CCM (N) < SDM (N), CCM (H+G) < SDM (H+G), and CCM (H–G) < SDM (H–G)] (Fig. 5).

The addition of TGF-β1 neutralizing Ab had little or no influence on the SCAP secretome-induced migration. Statistically significant reduction of HUVEC migration was observed only after blocking of the CCM (N) (reduction by 12.5% ± 11.1%), SDM (N) (reduction by 12.8% ± 10.1%), and SDM (H+G) (reduction by 21.2% ± 6.6%) secretomes ($P < 0.05$), which were actually the samples found to contain

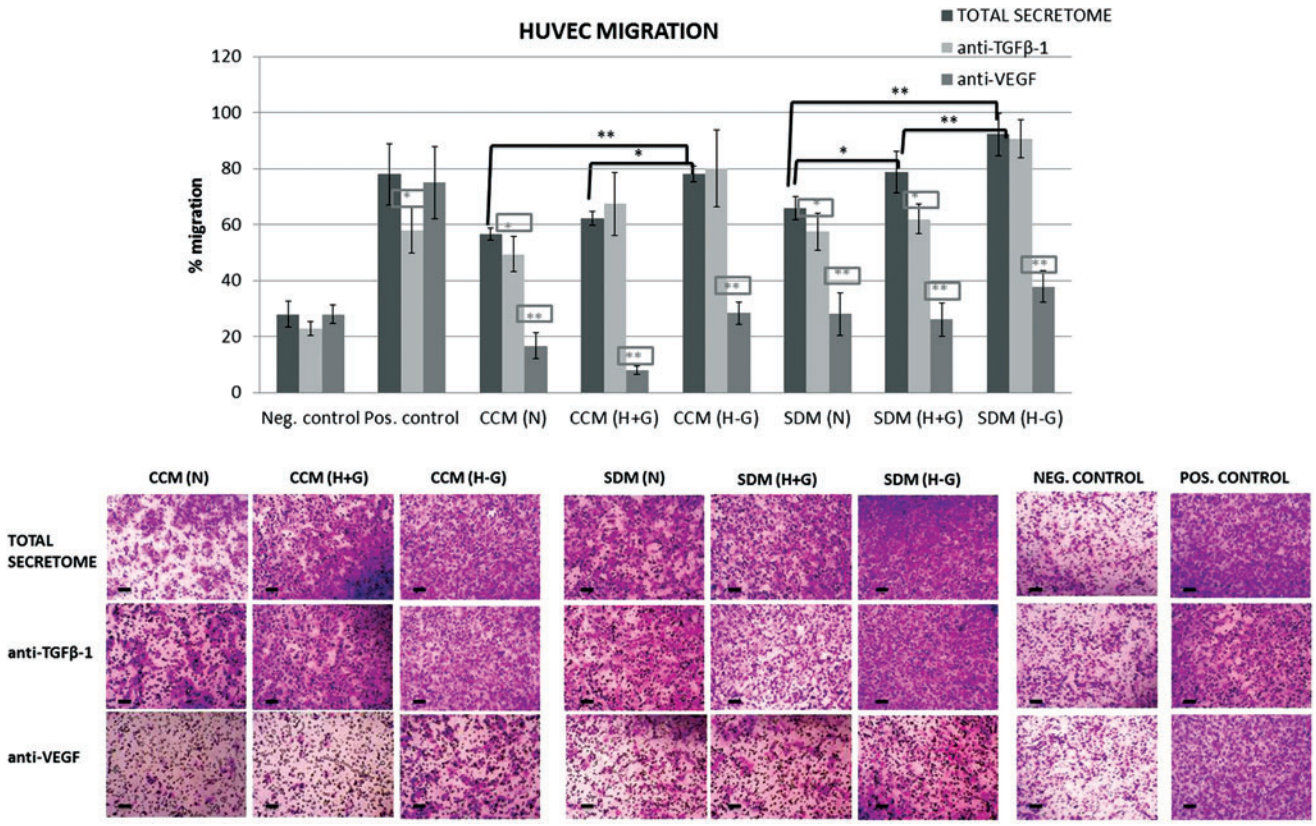

FIG. 5. Representative quantification data and light microscope microphotographs (scale bars 100 μm) of the in vitro transwell migration assay and respective blocking experiments, showing the percentage (%) of HUVEC migration after exposure to SCAP secretomes collected under different stress conditions (groups 1–6). Results are expressed as means ± standard deviations of three independent experiments in duplicates [*black asterisks* indicate statistically significant differences between N, H+G, and H–G conditions within the same serum concentration group, that is, CCM or SDM, and *gray asterisks* (in the rectangular frame) indicate statistically significant differences of each of the blocked (with anti-VEGF and anti-TGF-β1) secretomes compared with the total secretome within the same group, $*P < 0.05$, $**P < 0.01$]. Positive control: CCM (containing 15% FBS) and negative control: SDM (containing 2% FBS). Color images available online at www.liebertpub.com/scd

the highest amounts of TGF-β1, as shown by the ELISA colorimetric assay [Fig. 4B (b)]. In contrast, addition of VEGF neutralizing Ab dramatically reduced or almost completely inhibited HUVEC migration caused by all secretomes ($P < 0.01$). Migration was markedly reduced for the different conditions (secretomes) as follows: CCM (N) = 70.4% ± 8.3%, CCM (H+G) = 87.1% ± 2.5%, CCM (H–G) = 63.6% ± 5%, SDM (N) = 57.5% ± 11.3%, SDM (H+G) = 66.9% ± 7.6%, and SDM (H–G) = 58.8% ± 6%.

The second functional assay focused on the ability of SCAP secretome to induce vascular tubule formation by HUVECs. It was shown that the secretome collected under glucose/oxygen deprivation (GOD) conditions in the presence [G3: CCM (H–G)] or mainly in the absence of serum [G6: SDM (H–G)] was significantly more potent in inducing capillary network formation by HUVECs compared with that collected under less stressful microenvironments. The overall number of master junctions/field (268 ± 41.3), total number of master segments (501 ± 57), and total master segment length/field (46,542 ± 6,078 μm) in HUVEC cultures exposed to SDM (H–G) secretome were statistically significantly higher than those exposed to SDM (H+G) (number of junctions: 134 ± 10.7, number of segments: 247 ± 25, total segment length: 18,216 ± 4,826 μm) and SDM (N) (number of junctions: 147 ± 16.5, number of segments: 292 ± 40.5, total segment length: 21,103 ± 4,154 μm), respectively ($P < 0.01$). Moreover, one-way analysis of variance and Bonferroni's post hoc test revealed that the secretome collected under CCM conditions was a less potent inducer of capillary sprouting compared with that collected under SDM conditions only for the (N) and (H–G) groups, that is, CCM (N) < SDM (N) and CCM (H–G) < SDM (H–G) ($P < 0.05$) (Fig. 6).

Blocking with anti-VEGF Ab markedly reduced the tubule-forming potential of all secretomes [except G1: CCM (N) and G2: CCM (H+G)], while treatment with anti-TGF-β Ab had no effect on this assay (Fig. 6). Collectively, data from both functional assays suggest a paracrine proangiogenic effect of SCAP on HUVECs, which is enhanced when SCAP are exposed to stress microenvironments devoid of oxygen and nutrients, such as those encountered in damaged tissues.

Discussion

Dental tissue-derived MSCs have recently triggered worldwide interest as an attractive and easily accessible

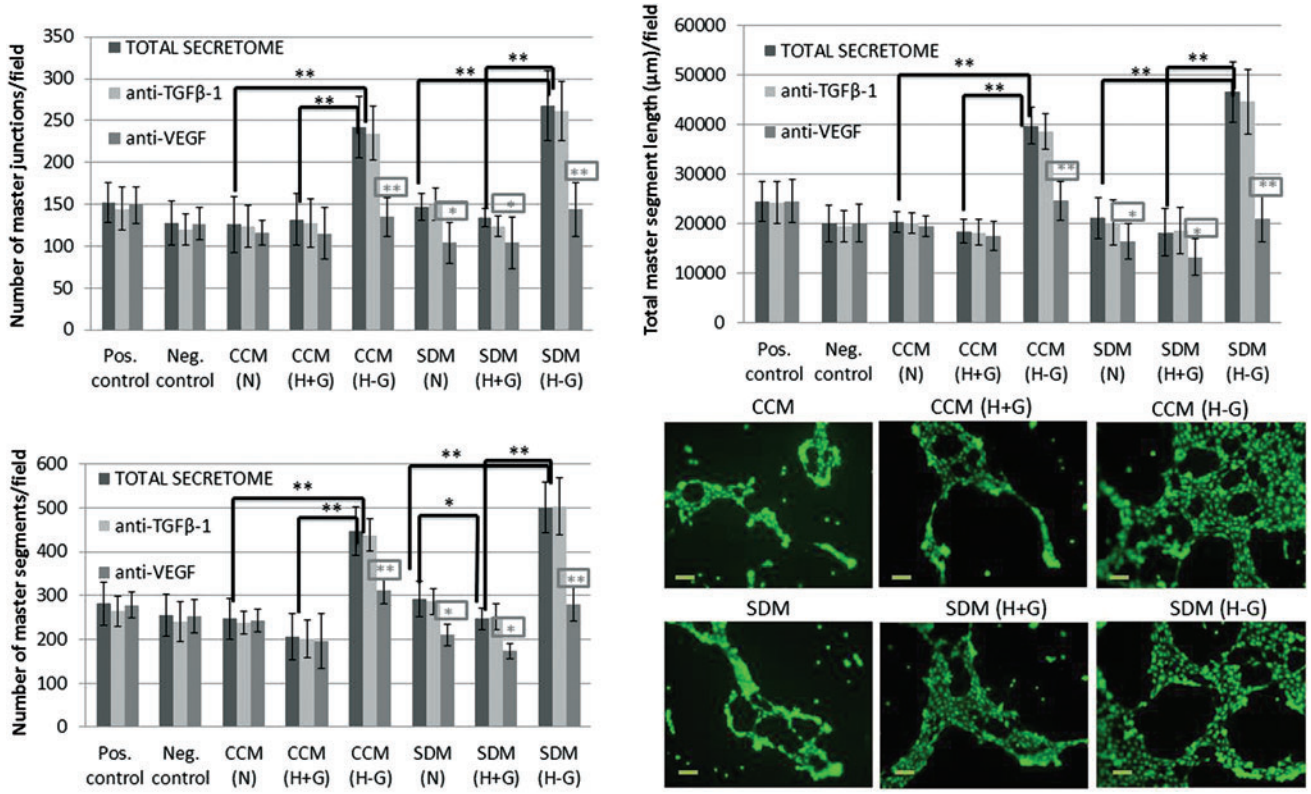

FIG. 6. Representative quantification data and light microscope microphotographs (scale bars 100 μm) of the in vitro capillary-like network formation assay and respective blocking experiments, showing the number of master junctions, number of master segments, and total master segment length after exposure of HUVECs to SCAP secretomes collected under different stress conditions (groups 1–6). Results are expressed as means ± standard deviations of three independent experiments in duplicates [*black asterisks* indicate statistically significant differences between N, H+G, and H–G conditions within the same serum concentration group, that is, CCM or SDM, and *gray asterisks* (in the rectangular frame) indicate statistically significant differences of each of the blocked (with anti-VEGF and anti-TGF-β1) secretomes compared with the total secretome within the same group, $*P < 0.05$, $**P < 0.01$]. Positive control: CCM (containing 15% FBS) and negative control: SDM (containing 2% FBS). Color images available online at www.liebertpub.com/scd

source of cells with angiogenic potential. In particular, stem cells derived from the heavily vascularized apical papilla of adult developing teeth (SCAP) seem to be a promising therapeutic tool for the regeneration of ischemic or damaged tissues. The immunophenotypic profiles of SCAP cultures (Fig. 1) reveal a very high expression of mesenchymal, endothelial, neural, and embryonic SC markers compared with other MSC sources, such as BM-MSCs [29] and DPSCs [15], suggesting a higher degree of stem cell enrichment [26,30] possibly related to an enhanced plasticity. In the present study, we systematically studied three different aspects defining the angiogenic potential of SCAP under various stress conditions pertaining to in vivo situations in damaged tissues. These aspects include (1) the endothelial transdifferentiation potential of SCAP that could potentially become an integral part of new blood vessels, (2) the secretion of pro- and antiangiogenic factors, and (3) the impact of this secretome (paracrine effect) on the motility and sprouting potential of ECs (HUVEC).

Previous studies have supported the differentiation potential of dental MSCs into ECs, as evidenced by upregulation of typical EC markers, such as PECAM-1, VEGFR-2, vWF, and VE-cadherin, and capillary-like structure formation on Matrigel or other matrices [19,20,31,32]. Recently, Bento et al. [20] showed the differentiation of SHED into VEGFR-2/CD31-positive EC-like cells through a VEGF/MEK1/ERK signaling pathway. Moreover, Cordeiro et al. [33] showed that SHED differentiated into ECs in vivo when seeded in biodegradable scaffolds and transplanted into immunodeficient mice. There is already extensive literature on the endothelial transdifferentiation potential of different types of MSCs. Interestingly, some of these studies used basal low serum (2%–5% FBS) media, supplemented with 50–100 ng/mL VEGF as a means of triggering endothelial shift of MSCs into ECs [7,8,19], while other studies are based on more complicated media, such as the endothelial growth medium-2/EGM-2, containing a cocktail of proangiogenic factors (VEGF, EGF, FGF-2, IGF-1, hydrocortisone, heparin, ascorbic acid, and 2% FCS), to achieve a more effective commitment of MSCs to ECs [20]. Indeed, some studies have shown that incubation of MSCs with basal media containing VEGF was not so effective in skewing MSCs to ECs [34]. The same observation was made in our system since preliminary experiments using aMEM containing 5%–15% FBS and 50–100 ng/mL VEGF showed that these media were not very potent in inducing endothelial transdifferentiation of SCAP (data not shown). This is the reason why a more complex medium containing

most of the above-mentioned (for EGM-2) supplements and growth factors was used in the present study. According to the results, continuous exposure of SCAP to this potent angiogenic medium for 28 days led to substantial time-dependent increase in expression of several angiogenesis-related molecules and to acquisition of a capillary-like-forming potential, both indicative of an EC-like phenotype (Fig. 2A–D). During this process, VEGFR-2 expression gradually increased, while VEGFR-1 expression was markedly suppressed over time. Sakai et al. [19] showed that VEGFR-1 is constitutively expressed by undifferentiated DPSCs, while Bento et al. [20] showed that VEGFR-1-silenced SHED showed less angiogenic potential in vivo than controls, suggesting that VEGFR-1 signaling allows for the initial commitment of dental MSCs into ECs, while VEGFR-2 mediates the full expression of the angiogenic effects of VEGF at a later stage.

Regarding the angiopoietins/Tie angiogenesis system, the present study demonstrated that endothelial transdifferentiation of SCAP was associated with significant upregulation of Ang-2 and Tie-1 and parallel downregulation of Ang-1 and Tie-2 expression. Both Ang-1 and -2 are ligands of the Tie-2 receptor, sharing the same binding sites [35]. Ang-1 is constitutively expressed by many cell types, such as pericytes, smooth muscle cells, and fibroblasts, while Ang-2 is mainly expressed by ECs and is upregulated at sites of angiogenesis as a response to positive regulators of its promoter activity, such as VEGF [35]. Based on these data, it is reasonable to assume that upregulation of Ang-2 in our system is a result of the endothelial transformation of SCAP in response to VEGF, while downregulation of Ang-1 and the receptor Tie-2 expression, which is initially abundant in undifferentiated SCAP, is probably a result of antagonistic function of Ang-2 activation. The latter is supported by studies showing that Ang-2 is able to inhibit Ang-1-mediated Tie-2 phosphorylation and activation in ECs [36]. A novel finding in this study was the significant upregulation of Tie-1 in the course of transdifferentiation of SCAP toward EC-like cells. Some studies support that Tie-1 activation does not occur in a ligand-dependent manner [37], while others propose Ang-1 to activate Tie-1 directly [38] or indirectly through Tie-2 activation [39]. Tie-1 may also interact with Tie-2, limiting Tie-2 responsiveness to Ang-1 [37,39]. Based on these data, it seems that Tie-1 is activated as a response to VEGF-induced endothelial transformation of SCAP, leading to antagonistic suppression of Ang-1/Tie-2 activity.

It has to be noted that despite upregulation of typical EC molecules, it remains questionable whether MSCs may finally acquire a mature and functional EC phenotype. In the present study, the steady-state mRNA levels of all respective EC markers in HUVECs far exceed that acquired during endothelial shift of SCAP (Fig. 2B). Flow cytometric analysis (Fig. 2C) indicates that a certain component of the heterogeneous SCAP population possesses the ability to differentiate toward an EC-like phenotype. However, further molecular research is necessary to define the various stages of endothelial transformation of an MSC up to a mature EC.

An interesting finding in our study was that short-term exposure (72 h) of SCAP to stressful microenvironments (ie, SD, OD, and GD individually or in combination) was equally or even more potent in eliciting a proangiogenesis process compared with exposure to the angiogenic medium for 28 days. This was particularly evident when combined GOD in CCM and—mainly—when SDM was applied (Fig. 3A). Moreover, SCAP showed high adaptability to these conditions, retaining high overall levels of cell viability and maintaining cellular morphology unchanged, while in case of GOD in presence or absence of serum, they acquired a typical capillary-forming EC phenotype (Fig. 3B). Previous in vitro and in vivo studies reported increased MSC survival after preconditioning by cultivation under hypoxic and SD conditions [40]. Grayson et al. [41] reported that long-term (up to 24 days) culture of human MSCs under hypoxic (2% O_2) conditions resulted in decreased proliferation, but not increased apoptosis. Other studies support that in vitro MSC cultivation under normoxic conditions (20% O_2) deviates significantly from the physiological oxygen pressure (normoxia) encountered in various tissues, which normally ranges between 1% and 11% O_2 [42].

It has been also shown that hypoxia (1%–2% for 24–72 h) enhances the angiogenic potential of dental pulp cells [43] and triggers neoangiogenic processes by several MSC types [44] as an adaptive mechanism to ensure nutrient and oxygen supply to the injured tissues [40]. Hypoxia-induced angiogenesis is mainly mediated through activation of the family of HIFs that regulate the expression of nearly 200 genes controlling glucose uptake, metabolism, angiogenesis, erythropoiesis, cell proliferation, and apoptosis [44]. HIF is a heterodimeric protein of an oxygen-sensitive HIF-A subunit and a constitutive HIF-B subunit (also known as ARNT) [44]. Two isoforms of the HIF-A subunit (HIF-1A and HIF-2A) have been identified. HIF-1A has been related to the regulation of the most known hypoxia target genes, while less is known about the role of HIF-2A [45]. Studies suggest that HIF-1A is mainly transcriptionally active during the initial phase of acute hypoxia, while HIF-2A takes action at later, more chronic hypoxia phases [45]. In dental pulp cells, HIF-1A expression was shown to peak at 4 h of hypoxia and to decrease gradually through 24 h under normoxia [43], suggesting rapid degradation of this subunit after reoxygenation. In the present study, transcriptional upregulation was observed only for the HIF-2A and HIF-1B subunits, while HIF-1A was found to be downregulated after 72 h of exposure to hypoxic (with or w/o glucose) conditions. This can be explained by the above-mentioned experimental data supporting upregulation of HIF-1A only during the first few hours of hypoxia and needs further investigation.

SD has been shown to have contradictory effects on various cell types, depending on exposure, length, and serum concentration [46]. Some studies report induction of massive cell death in the form of apoptosis after intensive and long-term exposure to SD and/or hypoxia [47]. Other studies show that MSCs may survive long-term SD and/or hypoxia, maintaining their normal morphology [40], as also shown in our study. MSCs present metabolic flexibility as they can survive by secretion of several prosurvival and angiogenic factors that may act in an autocrine or paracrine manner [9,48]. In the absence of oxygen, MSCs may survive using anaerobic ATP production through glycolysis rather than rely on mitochondria respiration [48]. Finally, in cases of both GOD, cells may use ketogenic amino acid-, fatty acid-, or ketone body-derived acetyl-CoA for the citric acid cycle to supply NADH_H_/$FADH_2$ to fuel the terminal oxidation [48]. In the present study, stress factors were

compared to assess their potency in promoting endothelial transdifferentiation of dental MSCs (SCAP). A combination of serum, glucose, and oxygen (SGOD) deprivation for 72 h was used to imitate conditions of harsh ischemia in vivo. It was noteworthy that these conditions not only rapidly increased expression of all angiogenesis-related markers but also induced an obvious change in phenotype to lumen-forming cells, indicative of an endothelial shift. The same phenomenon was observed in GOD cultures in the presence of serum-containing medium [CCM (H–G)], but not in cultures exposed to hypoxia in the presence of glucose (H+G) either under CCM or SDM conditions, suggesting that the critical microenvironmental condition for inducing a rapid angiogenic shift of SCAP is the combination of GD and OD, acting more effectively when SD is also present. To the best of our knowledge, this is the first study reporting survival and rapid endothelial shift of MSCs under extended conditions of SGOD.

These results are fully supported by the findings obtained from the SCAP secretome analysis using proteome profiler and ELISA assays (Fig. 4A, B). A higher number of secreted factors was detected under conditions of combined SGOD ($n=22$) compared with SOD ($n=10$) or SD ($n=17$) alone. Moreover, higher relative amounts of proangiogenic factors (angiogenin, IGFBP-3, and VEGF) and lower amounts of antiangiogenic molecules (serpin-E1, TIMP-1, TSP-1) were released under SGOD compared with SOD or SD alone ($P<0.05$). These data confirm that the secretome composition may change significantly in dynamic cross talk with the local microenvironment. Despite the disparate secretome profiles obtained under various stress conditions, the molecules angiogenin, Ang-1, IGFBP-3, uPA, VEGF (proangiogenic) and PTX-3, serpin-E1, -F1, TIMP-1, and TSP-1 (antiangiogenic) were detected in all cases. Under normoxia (N) in the presence of SD, the molecules CXCL-16, IGFBP-2, HGF, PIGF, MCP-1, FGF-7, and TIMP-4 were additionally secreted. These results are in close agreement with a recent study by Hilkens et al. [24], who found similar factors secreted in SCAP CM collected after 48 h of SD (0.1% FBS).

Among the detected proangiogenic factors, angiogenin has been shown to interact with ECs to induce migration, proliferation, and tube formation [49], Ang-1 plays a role in tubulogenesis and vessel stabilization [50], while IGFBP-3 not only stimulates endothelial motility but may also downregulate proangiogenic factors, such as VEGF and bFGF acting in an opposing manner [51]. VEGF is considered as the most potent mediator of neoangiogenesis, regulating endothelial proliferation, migration, sprouting formation, and vasodilation [50]. ELISA confirmed in this study that exposure of SCAP to hypoxic conditions (with or w/o GD) significantly increased VEGF secretion, which can be justified as being a major target gene of HIF-1 activation, as explained above. In contrast, FGF-2 could be detected at minimal levels in SCAP secretome under all conditions. This is in accordance with Bronckaers et al. [23] who found that FGF-2 was abundantly present in DPSC lysates, but was not secreted into the medium, as well as with Aranha et al. [43] who found that hypoxia elevates secretion of VEGF, but not FGF-2, in DPSC cultures. Finally, uPA, which belongs to the serine proteases family, catalyzes plasminogen to plasmin, which is involved in proteolysis and activation of MMPs and growth factors, promoting EC invasion [52]. Antiangiogenic factors, on the other hand, comprise a heterogeneous group of molecules, acting primarily through their ability to bind and sequester proangiogenic factors, thus blocking their interaction with ECs [50]. The equilibrium between angiogenic stimulators and inhibitors in the microenvironment, the so-called angiogenic balance, tightly controls the rate of blood vessel formation under physiological conditions, while a switch occurs in various pathologies.

Since both pro- and antiangiogenic factors were detected in SCAP secretome, functional assays were performed to assess whether the angiogenic balance is shifted toward neoangiogenesis or, in contrast, its inhibition. Both functional assays showed that secretome obtained under combined SGOD conditions was the most effective in inducing migration and vascular tubule formation by HUVECs (Figs. 5 and 6), therefore confirming its beneficial proangiogenic properties. Furthermore, to validate the potency of individual soluble mediators in SCAP secretome, blocking experiments were performed. We have shown that blocking of VEGF was sufficient to effectively eliminate its proangiogenic effects, highlighting the central role of VEGF secretion in the proangiogenic properties of MSCs. In contrast, the angiogenic activity induced by SCAP secretome was not significantly attenuated by the neutralizing antibody for TGF-β1. TGF-β1 is an important cytokine that promotes angiogenesis, at least in part, through the secretion of the survival factors, TGF-α and VEGF, which activate PI3K/Akt and MAPK pathways [53]. A potential explanation for the restricted effects of TGF-β1 blocking rests in the results of the ELISA showing a decreased release of TGF-β1 under (H–G) compared with (H+G) and (N) conditions. In accordance with this, statistically significant reduction of the HUVEC migration rate was observed only after blocking of those samples containing the higher amounts of TGF-β1 [CCM (N), SDM (N), and SDM (H+G)] (Fig. 4B). These results show that despite the undisputable biological role of TGF-β1 in inducing migration of various cell types [28], its presence in SCAP secretome obtained under conditions of severe environmental stress (SGOD) is not dominant compared with other proangiogenic factors. No differences were also obtained in the tubule formation assay after TGF-β1 blocking. These results are in accordance with a recent study by Kwon et al. [54] who showed that blocking of VEGF, MCP-1, and IL-6, but not of TGF-β1 and HGF, could suppress the angiogenic properties of MSC secretome.

In summary, the present study highlights the complexity of MSC responses to environmental cues present in damaged tissues and provides new insights into dental MSC preconditioning strategies aiming to improve their therapeutic potential. In particular, it was shown that SCAP endothelial transdifferentiation potential as well as angiogenic paracrine activity was profoundly enhanced when exposed for a short time to combined SGOD conditions. These results also underline the remarkable adaptability of dental MSCs in conditions of harsh environmental stress, which renders them an attractive cell source for the regenerative management of damaged/ischemic tissues. There is also significant benefit toward developing regeneration strategies for various clinical applications in dental pathology, including pulp, periodontal ligament, and bone regeneration. Further studies will validate the in vivo angiogenic therapeutic potential of SCAP and their secretome under targeted preconditioning strategies in a dynamic cross talk with the local microenvironment.

Acknowledgments

The study was supported by a research grant from the Alexander S. Onassis Public Benefit Foundation awarded to Dr. A. Bakopoulou. The authors would also like to thank Mrs. Angela Beckedorf for her excellent technical assistance.

Author Disclosure Statement

No competing financial interests exist.

References

1. Carmeliet P. (2000). Mechanisms of angiogenesis and arteriogenesis. Nat Med 6:389–395.
2. Laschke MW, Y Harder, M Amon, I Martin, J Farhadi, A Ring, N Torio-Padron, R Schramm, M Rücker, et al. (2006). Angiogenesis in tissue engineering: breathing life into constructed tissue substitutes. Tissue Eng 12:2093–2104.
3. About I. (2014). Pulp vascularization and its regulation by the microenvironment. In: *The Dental Pulp*. Goldberg M, ed. Springer-Verlag, Heidelberg, pp 61–74.
4. Carmeliet P and RK Jain. (2011). Molecular mechanisms and clinical applications of angiogenesis. Nature 473:298–307.
5. Ribatti D and E Crivellato. (2012). ''Sprouting angiogenesis'', a reappraisal. Dev Biol 372:157–165.
6. Potente M, H Gerhardt and P Carmeliet. (2011). Basic and therapeutic aspects of angiogenesis. Cell 146:873–887.
7. Jazayeri M, A Allameh, M Soleimani, SH Jazayeri, A Piryaei and S Kazemnejad. (2008). Molecular and ultrastructural characterization of endothelial cells differentiated from human bone marrow mesenchymal stem cells. Cell Biol Int 32:1183–1192.
8. Oswald J, S Boxberger, B Jørgensen, S Feldmann, G Ehninger, M Bornhäuser and C Werner. (2004). Mesenchymal stem cells can be differentiated into endothelial cells in vitro. Stem Cells 22:377–384.
9. Oskowitz A, H McFerrin, M Gutschow, ML Carter and R Pochampally. (2011). Serum-deprived human multipotent mesenchymal stromal cells (MSCs) are highly angiogenic. Stem Cell Res 6:215–225.
10. Ranganath SH, O Levy, MS Inamdar and JM Karp. (2012). Harnessing the mesenchymal stem cell secretome for the treatment of cardiovascular disease. Cell Stem Cell 10: 244–258.
11. Chuang TJ, KC Lin, CC Chio, CC Wang, CP Chang and JR Kuo. (2012). Effects of secretome obtained from normoxia-preconditioned human mesenchymal stem cells in traumatic brain injury rats. J Trauma Acute Care Surg 73:1161–1167.
12. Ando Y, K Matsubara, J Ishikawa, M Fujio, R Shohara, H Hibi, M Ueda and A Yamamoto. (2014). Stem cell-conditioned medium accelerates distraction osteogenesis through multiple regenerative mechanisms. Bone 261:82–90.
13. Chen L, EE Tredget, PY Wu and Y Wu. (2008). Paracrine factors of mesenchymal stem cells recruit macrophages and endothelial lineage cells and enhance wound healing. PLoS One 3:e1886.
14. Janebodin K, Y Zeng, W Buranaphatthan, N Ieronimakis and M Reyes. (2013). VEGFR2-dependent angiogenic capacity of pericyte-like dental pulp stem cells. J Dent Res 92:524–531.
15. Egusa H, W Sonoyama, M Nishimura, I Atsuta and K Akiyama. (2012). Stem cells in dentistry—part I: stem cell sources. J Prosthodont Res 56:151–165.
16. Shi S and S Gronthos. (2003). Perivascular niche of postnatal mesenchymal stem cells in human bone marrow and dental pulp. J Bone Miner Res 18:696–704.
17. Dissanayaka WL, X Zhan, C Zhang, KM Hargreaves, L Jin and EH Tong. (2012). Coculture of dental pulp stem cells with endothelial cells enhances osteo-/odontogenic and angiogenic potential in vitro. J Endod 38:454–463.
18. Yuan C, P Wang, L Zhu, WL Dissanayaka, DW Green, EH Tong, L Jin and C Zhang. (2015). Coculture of stem cells from apical papilla and human umbilical vein endothelial cell under hypoxia increases the formation of three-dimensional vessel-like structures in vitro. Tissue Eng Part A 21:1163–1172.
19. Sakai VT, Z Zhang, Z Dong, KG Neiva, MA Machado, S Shi, CF Santos and JE Nör. (2010). SHED differentiate into functional odontoblasts and endothelium. J Dent Res 89: 791–796.
20. Bento LW, Z Zhang, A Imai, F Nör, Z Dong, S Shi, FB Araujo and JE Nör. (2013). Endothelial differentiation of SHED requires MEK1/ERK signaling. J Dent Res 92:51–57.
21. Gandia C, A Armiña, JM García-Verdugo, E Lledó, A Ruiz, MD Miñana, J Sanchez-Torrijos, R Payá, V Mirabet, et al. (2008). Human dental pulp stem cells improve left ventricular function, induce angiogenesis, and reduce infarct size in rats with acute myocardial infarction. Stem Cells 26:638–645.
22. Ishizaka R, Y Hayashi, K Iohara, M Sugiyama, M Murakami, T Yamamoto, O Fukutaa and M Nakashima. (2013). Stimulation of angiogenesis, neurogenesis and regeneration by side population cells from dental pulp. Biomaterials 34:1888–1897.
23. Bronckaers A, P Hilkens, Y Fanton, T Struys, P Gervois, C Politis, W Martens and I Lambrichts. (2013). Angiogenic properties of human dental pulp stem cells. PLoS One 8: e71104.
24. Hilkens P, Y Fanton, W Martens, P Gervois, T Struys, C Politis, I Lambrichts and A Bronckaers. (2014). Pro-angiogenic impact of dental stem cells in vitro and in vivo. Stem Cell Res 12:778–790.
25. About I. (2013). Dentin–pulp regeneration: the primordial role of the microenvironment and its modification by traumatic injuries and bioactive materials. Endodontic Topics 28:61–89.
26. Bakopoulou A, G Leyhausen, J Volk, A Tsiftsoglou, P Garefis, P Koidis and W Geurtsen. (2011). Comparative analysis of in vitro osteo/odontogenic differentiation potential of human dental pulp stem cells (DPSCs) and stem cells from the apical papilla (SCAP). Arch Oral 56:709–21.
27. Rasband WS. (1997–2014). Image J. U.S. National Institutes of Health, Bethesda, MD. http://imagej.nih.gov/ij/
28. Evrard SM, C d'Audigier, L Mauge, D Israël-Biet, CL Guerin, I Bieche, JC Kovacic, AM Fischer, P Gaussem and DM Smadja. (2012). The profibrotic cytokine transforming growth factor-β1 increases endothelial progenitor cell angiogenic properties. J Thromb Haemost 10:670–679.
29. Lv FJ, RS Tuan, KM Cheung and VY Leung. (2014). Concise review: the surface markers and identity of human mesenchymal stem cells. Stem Cells 32:1408–1419.
30. Bianco P, PG Robey and PJ Simmons. (2008). Mesenchymal stem cells: revisiting history, concepts, and assays. Cell Stem Cell 2:313–319.
31. Iohara K, L Zheng, H Wake, M Ito, J Nabekura, H Wakita, H Nakamura, T Into, K Matsushita and M Nakashima. (2008). A novel stem cell source for vasculogenesis in ischemia:

subfraction of side population cells from dental pulp. Stem Cells 26:2408–2418.
32. Marchionni C, L Bonsi, F Alviano, G Lanzoni, A Di Tullio, R Costa, M Montanari, PL Tazzari, F Ricci, et al. (2009). Angiogenic potential of human dental pulp stromal (stem) cells. Int J Immunopathol Pharmacol 22:699–706.
33. Cordeiro MM, Z Dong, T Kaneko, Z Zhang, M Miyazawa, S Shi, AJ Smith and JE Nör. (2008). Dental pulp tissue engineering with stem cells from exfoliated deciduous teeth. J Endod 34:962–969.
34. Roobrouck VD, C Clavel, SA Jacobs, F Ulloa-Montoya, S Crippa, A Sohni, SJ Roberts, FP Luyten, SW Van Gool, et al. (2011). Differentiation potential of human postnatal mesenchymal stem cells, mesoangioblasts, and multipotent adult progenitor cells reflected in their transcriptome and partially influenced by the culture conditions. Stem Cells 29:871–882.
35. Fiedler U, Y Reiss, M Scharpfenecker, V Grunow, S Koidl, G Thurston, NW Gale, M Witzenrath, S Rosseau, et al. (2006). Angiopoietin-2 sensitizes endothelial cells to TNF-alpha and has a crucial role in the induction of inflammation. Nat Med 12:235–239.
36. Scharpfenecker M, U Fiedler, Y Reiss and HG Augustin. (2005). The Tie-2 ligand angiopoietin-2 destabilizes quiescent endothelium through an internal autocrine loop mechanism. J Cell Sci 118:771–780.
37. Marron MP, H Singh, TA Tahir, J Kavumkal, HZ Kim, GY Koh and NP Brindle. (2007). Regulated proteolytic processing of Tie1 modulates ligand responsiveness of the receptor-tyrosine kinase Tie2. J Biol Chem 282:30509–30517.
38. Saharinen P, K Kerkela, N Ekman, M Marron, N Brindle, GM Lee, H Augustin, GY Koh and K Alitalo. (2005). Multiple angiopoietin recombinant proteins activate the Tie1 receptor tyrosine kinase and promote its interaction with Tie2. J Cell Biol 169:239–243.
39. Yuan HT, S Venkatesha, B Chan, U Deutsch, T Mammoto, VP Sukhatme, AS Woolf and SA Karumanchi. (2007). Activation of the orphan endothelial receptor Tie1 modifies Tie2-mediated intracellular signaling and cell survival. FASEB J 21:3171–3183.
40. Amiri F, A Jahanian-Najafabadi and MH Roudkenar. (2015). In vitro augmentation of mesenchymal stem cells viability. Cell Stress Chaperones 20:237–251.
41. Grayson WL, F Zhao, B Bunnell and T Ma. (2007). Hypoxia enhances proliferation and tissue formation of human mesenchymal stem cells. Biochem Biophys Res Commun 358:948–953.
42. Carreau A, B El Hafny-Rahbi, A Matejuk, C Grillon and C Kieda. (2011). Why is the partial oxygen pressure of human tissues a crucial parameter? Small molecules and hypoxia. J Cell Mol Med 15:1239–1253.
43. Aranha AM, Z Zhang, KG Neiva, CA Costa, J Hebling and JE Nor. (2010). Hypoxia enhances the angiogenic potential of human dental pulp cells. J Endod 36:1633–1637.
44. Loor G and PT Schumacker. (2008). Role of hypoxia-inducible factor in cell survival during myocardial ischemia-reperfusion. Cell Death Differ 15:686–690.
45. Holmquist-Mengelbier L, E Fredlund, T Löfstedt, R Noguera, S Navarro, H Nilsson, A Pietras, J Vallon-Christersson, A Borg, et al. (2006). Recruitment of HIF-1alpha and HIF-2alpha to common target genes is differentially regulated in neuroblastoma: HIF-2alpha promotes an aggressive phenotype. Cancer Cell 10:413–423.
46. Roubelakis MG, G Tsaknakis, KI Pappa, NP Anagnou and SM Watt. (2013). Spindle shaped human mesenchymal stem/stromal cells from amniotic fluid promote neovascularization. PLoS One 8:e54747.
47. Potier E, E Ferreira, A Meunier, L Sedel, D Logeart-Avramoglou and H Petite. (2007). Prolonged hypoxia concomitant with serum deprivation induces massive human mesenchymal stem cell death. Tissue Eng 13:1325–1331.
48. Mylotte LA, AM Duffy, M Murphy, T O'Brien, A Samali, F Barry and E Szegezdi. (2008). Metabolic flexibility permits mesenchymal stem cell survival in an ischemic environment. Stem Cells 26:1325–1336.
49. Liu XH, CG Bai, ZY Xu, SD Huang, Y Yuan, DJ Gong and JR Zhang. (2008). Therapeutic potential of angiogenin modified mesenchymal stem cells: angiogenin improves mesenchymal stem cells survival under hypoxia and enhances vasculogenesis in myocardial infarction. Microvasc Res 76:23–30.
50. Distler JH, A Hirth, M Kurowska-Stolarska, RE Gay, S Gay and O Distler. (2003). Angiogenic and angiostatic factors in the molecular control of angiogenesis. Q J Nucl Med 47:149–161.
51. Granata R, L Trovato, E Lupia, G Sala, F Settanni, G Camussi, R Ghidonia and E Ghigo. (2007). Insulin-like growth factor binding protein-3 induces angiogenesis through IGF-I- and SphK1-dependent mechanisms. J Thromb Haemost 5: 835–845.
52. Raghu H, SS Lakka, CS Gondi, S Mohanam, DH Dinh, M Gujrati and JS Rao. (2010). Suppression of uPA and uPAR attenuates angiogenin mediated angiogenesis in endothelial and glioblastoma cell lines. PLoS One 5:e12458.
53. Viñals F and J Pouysségur. (2001). Transforming growth factor beta1 (TGF-beta1) promotes endothelial cell survival during in vitro angiogenesis via an autocrine mechanism implicating TGF-alpha signaling. Mol Cell Biol 21:7218–7230.
54. Kwon HM, SM Hur, KY Park, CK Kim, YM Kim, HS Kim, HC Shin, MH Won, KS Ha, et al. (2014). Multiple paracrine factors secreted by mesenchymal stem cells contribute to angiogenesis. Vasc Pharmacol 63:19–28.

Address correspondence to:
Dr. Athina Bakopoulou
Department of Fixed Prosthesis and Implant Prosthodontics
School of Dentistry
Aristotle University of Thessaloniki
Thessaloniki GR-54124
Greece

E-mail: abakopoulou@dent.auth.gr

Received for publication June 7, 2015
Accepted after revision July 21, 2015
Prepublished on Liebert Instant Online July 23, 2015